

Metagenomic analysis and metabolite profiling of deep-sea sediments from the Gulf of Mexico following the Deepwater Horizon oil spill

Nikole Elizabeth Kimes, Amy V. Callaghan, Deniz Atkas, Jan Sunner, Bernard T. Golding, Marta Drozdowska, Terry C. Hazen, Joseph Michael Suflita and Pamela J. Morris

Journal Name: Frontiers in Microbiology

ISSN: 1664-302X

Article type: Original Research Article

Received on: 17 Dec 2012

Accepted on: 21 Feb 2013

Provisional PDF published on: 21 Feb 2013

Frontiers website link: www.frontiersin.org

Citation: Kimes NE, Callaghan AV, Atkas D, Sunner J, Golding BT, Drozdowska M, Hazen TC, Suflita JM and Morris PJ(2013) Metagenomic analysis and metabolite profiling of deep-sea sediments from the Gulf of Mexico following the Deepwater Horizon oil spill. 4:50. doi:10.3389/fmicb.2013.00050

Article URL: http://www.frontiersin.org/Journal/Abstract.aspx?s=678&name=microbiological%20chemistry&ART_DOI=10.3389/fmicb.2013.00050

(If clicking on the link doesn't work, try copying and pasting it into your browser.)

Copyright statement: © 2013 Kimes, Callaghan, Atkas, Sunner, Golding, Drozdowska, Hazen, Suflita and Morris. This is an open-access article distributed under the terms of the [Creative Commons Attribution License](http://creativecommons.org/licenses/by/2.0/), which permits use, distribution and reproduction in other forums, provided the original authors and source are credited and subject to any copyright notices concerning any third-party graphics etc.

This Provisional PDF corresponds to the article as it appeared upon acceptance, after rigorous peer-review. Fully formatted PDF and full text (HTML) versions will be made available soon.

1 **Metagenomic analysis and metabolite profiling of deep-sea**
2 **sediments from the Gulf of Mexico following the Deepwater Horizon**
3 **oil spill**

4
5 **Contributors:** Nikole E. Kimes^{1#}, Amy V. Callaghan², Deniz F. Aktas^{2,3}, Jan Sunner^{2,3}, Bernard
6 T. Golding⁴, Marta Drozdowska⁴, Terry C. Hazen^{5,6}, Joseph M. Suflita^{2,3} and Pamela J. Morris^{1*}
7

8 ¹Belle W. Baruch Institute for Marine and Coastal Sciences, University of South Carolina,
9 Georgetown, SC, USA

10 ²Department of Microbiology and Plant Biology, University of Oklahoma, Norman, OK, USA

11 ³Institute for Energy and the Environment, University of Oklahoma, Norman, OK, USA

12 ⁴School of Chemistry, Bedson Building, Newcastle University, Newcastle upon Tyne, UK

13 ⁵Department Civil & Environmental Engineering, Microbiology, and Earth & Planetary
14 Sciences, University of Tennessee, Knoxville, TN, USA

15 ⁶Ecology Department, Lawrence Berkeley National Laboratory, Berkeley, CA, USA
16

17 **Correspondence:**

18 Dr. Pamela J. Morris

19 Belle W. Baruch Institute for Marine and Coastal Sciences

20 Baruch Marine Field Laboratory

21 University of South Carolina

22 PO BOX 1630

23 Georgetown, SC 29442

24 +001 843 991 8355

25 pjmorris@belle.baruch.sc.edu
26

27 [#]Current address: Evolutionary Genomics Group, División de Microbiología, Universidad
28 Miguel Hernández, San Juan, Alicante, Spain
29

30 **Running Title** (5 words): Gulf of Mexico deep-sea sediment metagenomics
31

32 **Keywords** (1-8): Deepwater Horizon/Metagenomics/Metabolomics/Oil-degradation
33

34 **Words:** 5300

35 **Figures and Tables:** 14 (10 figures and 2 tables in the text, 2 supplemental tables)
36

37 **ABSTRACT**

38 Marine subsurface environments, such as deep-sea sediments, house abundant and diverse
39 microbial communities that are believed to influence large-scale geochemical processes. These
40 processes include the biotransformation and mineralization of numerous petroleum constituents.
41 Thus, microbial communities in the Gulf of Mexico are thought to be responsible for the intrinsic
42 bioremediation of crude oil released by the Deepwater Horizon (DWH) oil spill. While
43 hydrocarbon contamination is known to enrich for aerobic, oil-degrading bacteria in deep-
44 seawater habitats, relatively little is known about the response of communities in deep-sea
45 sediments, where low oxygen levels may hinder such a response. Here, we examined the
46 hypothesis that increased hydrocarbon exposure results in an altered sediment microbial
47 community structure that reflects the prospects for oil biodegradation under the prevailing
48 conditions. We explore this hypothesis using metagenomic analysis and metabolite profiling of
49 deep-sea sediment samples following the DWH oil spill. The presence of aerobic microbial
50 communities and associated functional genes was consistent among all samples, whereas, a
51 greater number of Deltaproteobacteria and anaerobic functional genes were found in sediments
52 closest to the DWH blowout site. Metabolite profiling also revealed a greater number of putative
53 metabolites in sediments surrounding the blowout zone relative to a background site located 127
54 km away. The mass spectral analysis of the putative metabolites revealed that alkylsuccinates
55 remained below detection levels, but a homologous series of benzylsuccinates (with carbon chain
56 lengths from 5 to 10) could be detected. Our findings suggest that increased exposure to
57 hydrocarbons enriches for Deltaproteobacteria, which are known to be capable of anaerobic
58 hydrocarbon metabolism. We also provide evidence for an active microbial community
59 metabolizing aromatic hydrocarbons in deep-sea sediments of the Gulf of Mexico.
60

61 INTRODUCTION

62 The Deepwater Horizon (DWH) blowout resulted in the largest marine US oil spill to date, in
63 which 4.1 million barrels of crude oil flowed into the depths (~1500 m) of the Gulf of Mexico
64 (Operational Science Advisory Team, 2010). Although an estimated 78% of the oil was depleted
65 through either human intervention or natural means by August 2010 (Ramseur, 2010), the fate of
66 the remaining 22% was uncertain. Evidence subsequently showed that both oil (Hazen et al.,
67 2010; Mason et al., 2012) and gas (Kessler et al., 2011) persisted in the Gulf of Mexico water
68 column, affecting deep-sea (>1000 m) microbial communities that potentially facilitate the
69 biodegradation of residual hydrocarbons. Much less is known about the impact of
70 anthropogenic hydrocarbons on the microbial communities of deep-sea sediments. Although
71 much of the hydrocarbons from sub-sea oil spills and natural seeps may rise to the surface, there
72 are water-soluble components in oil as well as hydrocarbons adhering to solid particulates that
73 can settle in deep-sea sediments (Ramseur, 2010). After the 1979 Ixtoc I oil spill, for example,
74 in which over three million barrels of oil flowed into the Gulf of Mexico, it is estimated that 25%
75 of the oil was transported to the sea floor (Jernelov and Linden, 1981).

76
77 The deep-sea biosphere, including deep-sea sediments, is both one of the largest and one of the
78 most understudied ecosystems on earth (Jørgensen, 2011). Although the global estimates of
79 prokaryotic biomass supported by deep-subsurface sediments are lower than originally thought,
80 regional variation supports the presence of abundant and diverse seafloor microbial
81 communities in continental shelf areas, such as the Gulf of Mexico (Kallmeyer et al., 2012). This
82 is especially true for the more surficial sediment communities, such as those utilized in this
83 study. Evidence suggests that these deep-sea sediment communities support diverse metabolic
84 activities (D'Hondt et al., 2004; D'Hondt et al., 2009), including evidence of hydrocarbon
85 degradation in microbial communities associated with cold water hydrocarbon seeps located in
86 the Gulf of Mexico (Joye et al., 2004; Lloyd et al., 2006; Lloyd et al., 2010; Orcutt et al., 2010).
87 As a result, it has been suggested that the microbial communities in the Gulf of Mexico deep-sea
88 sediment would play a role in the biodegradation of persistent oil components following the
89 DWH blowout. Despite numerous advances pertaining to individual microorganisms capable of
90 metabolizing hydrocarbon compounds (Seth-Smith, 2010) and community responses to natural
91 hydrocarbon seeps (Lloyd et al., 2010; Orcutt et al., 2010), little is known about the microbial
92 capacity for oil-degradation within deep-sea sediment communities under the circumstances
93 presented by the DWH spill, including the extreme depth (~1500 m) and the sudden hydrocarbon
94 exposure.

95
96 To gain a better understanding of the sediment-associated microbial response to the DWH oil
97 spill, deep-sea sediment cores were collected by a Lawrence Berkeley National Laboratory
98 (LBNL) team aboard the R/V Gyre in the area surrounding the DWH oil spill between
99 September 19 and October 10, 2010. Preliminary chemical analysis revealed that the cores
100 closest to the DWH spill contained high levels of polycyclic aromatic hydrocarbons (PAHs)
101 (>24,000 µg/kg) compared to distant cores (~50 µg/kg), confirming a greater exposure of the
102 resident microflora to aromatic hydrocarbons near the DWH well (Operational Science Advisory
103 Team, 2010). Although it is likely that the DWH oil spill contributed to the higher PAH levels
104 observed, other sources that could have influenced these levels include natural seeps located near
105 the DWH site and drilling fluids.

106

107 In this study, we hypothesized that increased hydrocarbon exposure results in the alteration of
108 microbial community structure, such that it reflects the selection for organisms capable of the
109 anaerobic metabolism of petroleum constituents. We performed metagenomic sequencing on
110 three of the deep-sea sediment samples collected by LBNL (described above) and compared our
111 results to a Gulf of Mexico deep-subsurface sediment metagenomic library sequenced prior to
112 the DWH oil spill (Biddle et al., 2011). To complement the metagenomic analysis, metabolic
113 profiling was used to detect homologous series of putative signature metabolites associated with
114 anaerobic hydrocarbon biodegradation. Our data indicated significant differences among the
115 microbial communities examined in this study compared to those detected prior to the DWH oil-
116 spill. Moreover, the metabolite profiling revealed significantly more putative metabolites in the
117 two samples closest to the DWH site relative to the more distant background site. These findings
118 were consistent with the metagenomic data showing an increase in the number of functional
119 genes associated with anaerobic hydrocarbon degradation in samples closest to the DWH.

120

121 **MATERIALS AND METHODS**

122 **SAMPLE COLLECTION**

123 Deep-sea sediment cores were collected by LBNL from the area surrounding the Deepwater
124 Horizon oil spill in the Gulf of Mexico during six cruises by the R/V Gyre from September 16 to
125 October 20, 2010 (Operational Science Advisory Team, 2010). An OSIL Mega corer (Bowers &
126 Connelly) was used to collect deep-sea sediment cores, and overlying water was siphoned off
127 using a portable peristaltic pump. The capped sediment cores were frozen at -80°C and shipped
128 on dry ice to the LBNL where the cores were sectioned while frozen. The three cores utilized in
129 this study were designated SE-20101017-GY-D040S-BC-315 (GoM315); SE-20101017-GY-
130 D031S-BC-278 (GoM278); and SE-20100921-GY-FFMT4-BC-023 (GoM023). GoM315 and
131 GoM278 were located near the DWH well (0.5 and 2.7 km, respectively), while GoM023 was
132 located at a distance of 127 km from the DWH well (Figure 1). One half of each core (GoM315,
133 GoM278, and GoM023), approximately 5 in diameter and 1 in thick, was sent on dry ice to the
134 University of South Carolina Baruch Marine Field Laboratory in Georgetown, SC. Upon arrival
135 they were further subsectioned in half using sterile razorblades in a biosafety hood. One half
136 was used for DNA extraction and metagenomic analysis, while the other half was sent on dry ice
137 to the University of Oklahoma (Norman, OK) for metabolomic analysis.

138 **DNA EXTRACTION**

139 Inside a biosafety hood, a sterile razor blade was used to cut a 3-4 g wedge from each of the
140 three frozen cores (GoM315, GoM278, and GoM023). Community DNA was extracted from
141 each core using a PowerMax® Soil DNA Isolation kit (Mo Bio Laboratories, Inc., Carlsbad, CA)
142 according to the manufacturer's instructions. The resulting DNA (~ 2 µg) from each sample was
143 purified and concentrated via ethanol precipitation. The quality and quantity of the DNA were
144 assessed via gel electrophoresis on a 2% agar gel with a 1 kb ladder and spectrophotometer
145 analysis.

146 **METAGENOMIC SEQUENCING AND ANALYSIS**

147 Approximately 1 µg DNA (per core sample) was sent to Engencore (University of South
148 Carolina, Columbia, SC), where high-throughput sequencing was performed using the Roche
149 454 FLX pyrosequencing platform. The sequencing results were recorded as SFF files and
150 uploaded to the MetaGenome Rapid Annotation Subsystems Technology (MG-RAST) server for
151 analysis (Meyer et al., 2008). Each file underwent quality control (QC), which included quality

152 filtering (removing sequences with ≥ 5 ambiguous base pairs), length filtering (removing
153 sequences with a length ≥ 2 standard deviations from the mean), and dereplication (removing
154 similar sequences that are artifacts of shotgun sequencing). Organism and functional
155 identifications were made using a BLAT (BLAST-like alignment tool) search of the integrative
156 MG-RAST M5NR database, which is a non-redundant protein database that combines sequences
157 from multiple common sources. All identifications were made using a maximum e-value of $1e-5$,
158 a minimum identity cutoff of 50%, and a minimum alignment length of 50 bp. The
159 hierarchical clustering/heat map comparisons were constructed in MG-RAST using dendrograms
160 based on abundance counts for each category examined. Similarity/dissimilarity was determined
161 using a Euclidean distance metric, and the resulting distance matrix was combined with ward-
162 based clustering to produce dendrograms. Diversity indices for species richness and diversity
163 estimates were calculated using EstimateS software (Colwell, 2006). Circular recruitment plots
164 were created through the comparison of each metagenomic library to the whole genomes of
165 reference organisms (Refseq genomes only) using a maximum e-value of $1e-5$ and a \log_{10}
166 abundance scale. Three organisms of interest were investigated: *Alcanivorax borkumensis* SK2
167 (Yakimov et al., 1998; Schneiker et al., 2006; dos Santos et al., 2010), an aerobic
168 Gammaproteobacterium that utilizes oil hydrocarbons as its exclusive source of carbon and
169 energy and is often the most dominant bacterium in oil-polluted marine systems (Hara et al.,
170 2003; Harayama et al., 1999; Kasai et al., 2001; Yakimov et al., 2005), *Desulfatibacillum*
171 *alkenivorans* AK-01, a sulfate-reducing, *n*-alkane and *n*-alkene utilizing Deltaproteobacterium
172 (So and Young, 1999; Callaghan et al., 2012), and *Geobacter metallireducens* GS-15, a metal-
173 reducing, aromatic hydrocarbon utilizer within the *Deltaproteobacteria* (Lovley et al., 1993).

174 **PCR AMPLIFICATION OF FUNCTIONAL GENES**

175 Sediment DNA from GoM315, GoM278, GoM023 was also interrogated with nine primer set
176 combinations specific to *assA* and/or *bssA* (Callaghan et al., 2010). The *assA* and *bssA* genes
177 encode the catalytic subunits of the anaerobic glycyl radical enzymes, alkylsuccinate synthase
178 (ASS; also known as methylalkylsuccinate synthase, MAS) (Callaghan et al., 2008; Grundmann
179 et al., 2008) and benzylsuccinate synthase (BSS) (Leuthner et al., 1998), respectively. PCR
180 SuperMix (2X Dreamtaq, Fermentas) was used to set up 50- μ L reactions containing 25 μ L of 2X
181 Dreamtaq mastermix, 0.4 μ M of each primer, 5 μ L of betaine (5 M stock), and 10 ng of DNA
182 template. A modified touchdown PCR method (Muyzer et al., 1993) was used to minimize
183 unspecific amplification. The cycling program was as follows: 95°C for 4 minutes followed by
184 2 cycles at each annealing temperature (i.e., 95°C for 1 min, 63 to 52°C for one min, 72°C for
185 two min), 19 cycles at the plateau annealing temperature (53°C), and a final extension step at
186 72°C for 10 min.

187 **CONSTRUCTION AND PHYLOGENETIC ANALYSIS OF *assA* and *bssA* CLONE** 188 **LIBRARIES**

189 PCR products were purified using the Qiaquick purification kit (Qiagen) and cloned into either
190 pCRII or pCRII-TOPO vector (Invitrogen, Carlsbad, CA) following the manufacturer's
191 instructions. For each PCR product, colonies were picked into individual wells of two 96-well
192 microtiter plates and grown overnight. Inserts of the correct size were sequenced using the
193 M13R priming site. After sequencing, reads were trimmed to remove vector and primer
194 sequences before further analysis. Sequences from each respective library were assembled into
195 operational taxonomic units (OTUs) of $\geq 97\%$ sequence identity using Lasergene 7.2
196 (DNASTAR Inc., Madison, WI). The *assA/bssA* OTUs were aligned with *assA* and *bssA* genes
197 from described strains for which complete sequences were available and the best BLAST

198 matches (NCBI). Neighbor-joining trees were constructed in MEGA4 (Kumar et al., 2008) using
199 the Tajima Nei distance method, with pairwise deletion and performing 10,000 bootstrap
200 replicates. The glycol radical enzyme, pyruvate formate lyase (PFL), served as the outgroup. The
201 DNA sequences of GoM *assA* and *bssA* OTUs were deposited in GenBank under the accession
202 numbers JX135105 through JX135128.

203 **METABOLOMIC EXTRACTIONS AND ANALYSIS**

204 Approximately 25 g of each core sample was thawed in 20 ml of double-distilled sterile water
205 and then acidified with 10 N HCl until the pH was ≤ 2 . Each sample was mixed with 100 ml of
206 ethyl acetate and stirred overnight. The water phase was removed and the ethyl acetate solution
207 was dried over anhydrous Na₂SO₄, concentrated by rotary evaporation to approximately 2 mL
208 and reduced further under a stream of N₂ to a volume of 100 μ L. Half of the extract was
209 derivatized and analyzed by GC/MS as described previously (Aktas et al., 2010). The other half
210 was analyzed by LC/MS with an Agilent 1290 UPLC and an Agilent 6538 Accurate-Mass Q-
211 TOF with a dual ESI ion source. A 5 μ L volume of each concentrated ethyl acetate solution was
212 introduced to a ZORBAX SB-C18 column (2.1x100mm, 1.8 μ m). A gradient method was used
213 for the separation (0-3 min 15% acetonitrile, 3-25 min linear gradient to 95% acetonitrile in
214 water). The flow rate was 0.4 mL/min, and the temperature of the drying gas was maintained at
215 325°C. The data were analyzed using the Agilent B.04.00 MassHunter Qualitative Analysis
216 software. A positive identification of key metabolites, such as alkylsuccinates, alkylmalonates,
217 alkylbenzylsuccinates, and alkanolic acids, required that these were observed with the correct
218 mass (+/- 1 ppm), as well as with the retention times and MS/MS spectra observed for standard
219 compounds.

220

221 **RESULTS**

222 In total, we sequenced 191.6 Mb from three deep-sea sediment samples collected after the DWH
223 blowout (Table 1), which included two sediment cores (GoM315 and GoM278) within 3 km of
224 the DWH rig and one (GoM023) 127 km away (Figure 1). Post QC, 125.8 Mb were designated
225 as high-quality sequences (252,082 individual reads), resulting in an average of 84,023
226 individual reads (average length of 491 bp/read) per deep-sea sediment core (Table 1).

227 **PHYLOGENETIC CLASSIFICATION**

228 The MG-RAST classification tool revealed that at the domain level, all three samples had similar
229 distributions. Bacteria (97 – 95%) dominated, while the archaea (4.2 - 2.2%) and eukaryotes (0.8
230 – 0.6%) contributed substantially less to the sediment communities (Table 1). Differences
231 among the three samples were observed when examined at the phylum level (Figure 2). The
232 archaea associated with the deep-sea sediment cores were predominantly Euryarchaeota,
233 Thaumarchaeota, and Crenarchaeota (Figure 2A). The Euryarchaeota dominated (65%) in the
234 sample closest to the DWH rig (GoM315), but the same taxon and the Thaumarchaeota were
235 equally represented (45%) at GoM278. The Thaumarchaeota dominated (55%) in the sample
236 most distant from the spill site (GoM023).

237 Within the bacterial domain (Figure 2B), Proteobacteria dominated (60-65%) all three sediment
238 cores, followed by Firmicutes in GoM315 (9%), Bacteroidetes in GoM278 (11%), and
239 Actinobacteria in GoM023 (7%). The eukaryotic sequences represented 21 phyla from the
240 Animalia, Fungi, Plantae, and Protista kingdoms. The Animalia phyla Arthropoda (e.g., crab and
241 shrimp) and Chordata (e.g., fish and sharks) increased in abundance as the distance from the
242 DWH rig increased, while the Cnidaria (e.g., corals and sponges) and Nematoda (e.g.,

243 roundworms) phyla were found only at greater abundance in the two sediment cores closest to
244 the DWH rig. Although the number of viruses was relatively low (0.17 – 0.01%), a greater
245 number of viruses were associated with the two samples located nearest the DWH rig (GoM315
246 and GoM278) compared to the sample furthest away (Table 1). Alpha diversity values
247 calculated using annotated species-level distribution increased as the distance to the DWH rig
248 lessened. However, other diversity indices revealed similar levels of both species in richness and
249 diversity among the samples (Table 1).

250 The Proteobacteria associated with each sample were examined more closely in order to evaluate
251 the potential for both aerobic and anaerobic oil biodegradation (Figure 3), since numerous
252 Proteobacteria spp. are known to utilize petroleum hydrocarbons (Atlas, 1981; Widdel et al.,
253 2010). The Gammaproteobacteria was the most diverse class with the *Shewanella*,
254 *Marinobacter*, and *Pseudomonas* genera being the most common. Although the
255 Gammaproteobacteria were similarly distributed (~33%), the distributions of both the
256 Alphaproteobacteria and Deltaproteobacteria varied among the three deep-sea sediment samples
257 (Figure 3A). The Alphaproteobacteria, predominantly the Rhizobiales and Rhodobacterales
258 orders (Figure 3B), contributed to the highest percentage (37%) of Proteobacteria spp. in the
259 sample furthest from the DWH rig (GoM023), while the two closer samples (GoM315 and
260 GoM278) contained 30 and 26%, respectively. Greater numbers of sequences associated with
261 GoM023 were detected in numerous Alphaproteobacteria genera, including *Rhizobium*,
262 *Sinorhizobium*, *Bradyrhizobium*, *Roseobacter*, *Roseovarius*, and *Rhodobacter*.
263 Deltaproteobacterial distributions revealed a wider range than the Gamma- and
264 Alphaproteobacteria, one in which the two sediment cores closest to the DWH rig (GoM315 and
265 GoM278) exhibited higher levels (26 and 30% respectively), while the furthest core (GoM023)
266 exhibited only 16% Deltaproteobacteria (Figure 3A). No single organism accounted for the shift
267 in Deltaproteobacteria communities, rather a myriad of genera in the Desulfobacterales (e.g.,
268 *Desulfatibacillum*, *Desulfobacterium*, and *Desulfococcus*), Desulfovibrionales (e.g.,
269 *Desulfovibrio*), and Desulfuromonadales (e.g., *Geobacter*, and *Desulfomonas*) orders displayed
270 higher levels in the GoM315 and GoM278 samples (Figure 3B).

271 RECRUITMENT PLOTS

272 Recruitment plots, comparing sequences from each metagenomic library to the genomes of
273 specific organisms, supported the presence of known hydrocarbon-utilizing Proteobacteria
274 (Table 2). The analysis revealed a total of 169, 857, and 547 sequences, respectively, matching
275 to features of the *Alcanivorax borkumensis* SK2 genome [Proteobacteria; Gammaproteobacteria;
276 Oceanospirillales; Alcanivoracaceae] (Yakimov et al., 1998; Schneiker et al., 2006), the
277 *Desulfatibacillum alkenivorans* AK-01 genome [Proteobacteria; Deltaproteobacteria;
278 Desulfobacterales; Desulfobacteraceae] (So and Young, 1999; Callaghan et al., 2012), and the
279 *Geobacter metallireducens* GS-15 genome [Proteobacteria; Deltaproteobacteria;
280 Desulfuromonadales; Geobacteraceae] (Lovley et al., 1993) in all three deep-sea sediment
281 samples. Interestingly, matches to the aerobic hydrocarbon degrader, *A. borkumensis* SK2 (51-
282 61 sequence hits), remained consistent among all three samples; whereas, the comparison to the
283 two anaerobic hydrocarbon degraders, *D. alkenivorans* AK-01 (97-426 sequence hits) and *G.*
284 *metallireducens* GS-15 (92-278 sequence hits), revealed a greater number of sequence matches
285 to the two samples (GoM315 and GoM278) closest to the DWH well (Figure 4). Similarly,
286 sequences recruited to *Desulfococcus oleovorans* Hxd3 (Table 2), a model sulfate-reducing
287 alkane/alkene utilizer, in all three samples; however, GoM315 and GoM278 recruited a greater
288 number of sequences (256 and 332, respectively) compared to GoM023 (79).

289 **FUNCTIONAL GENE ANALYSIS**

290 All three samples revealed a similar functional blueprint at the broadest level of classification
291 (Figure 5A). Genes coding for clustering-based subsystems (15-16%), amino acid and
292 derivatives (9.2-9.3%), miscellaneous (8.2-9.5%), carbohydrates (8.8%), and protein metabolism
293 (7.4-8.7%) represented the five most abundant categories when classified using the SEED
294 database (Figure 5A). Analysis using COG classifications revealed a similar functional
295 distribution, with the majority of sequences assigned to metabolism (45-46%), followed by
296 cellular processes and signaling (19-21%), information storage and processing (17-18%), and
297 poorly characterized categories (15-18%). There was genetic evidence in all three samples for
298 the potential degradation of oil compounds, including genes vital to both the aerobic (e.g., mono-
299 and dioxygenases) and anaerobic degradation [e.g., benzylsuccinate synthase (*bss*) and benzoyl-
300 CoA reductase] of compounds such as butyrate, benzoate, toluene, and alkanolic acids
301 (Supplemental Table S1). Functional analysis of the “metabolism of aromatic compounds”
302 subsystem provided additional evidence of a greater potential for anaerobic metabolism in the
303 two samples nearest the DWH rig compared to the more distant sample (Figure 5B). GoM315
304 (located 0.5 km from the DWH rig) exhibited the highest percentage (15%) of anaerobic
305 degradation genes for aromatic compounds, while GoM023 (located 128 km from the DWH rig)
306 exhibited the lowest (9.9%). Notably, the metagenomics data revealed *bssA* in GoM315 only,
307 the sample closest to the DWH well, and the complete complement (subunits D-G) of benzoyl-
308 CoA reductase genes (Egland et al., 1997) was detected in GoM315 and GoM278, but not
309 GoM023, the site farthest from the DWH well.

310 **CLONE LIBRARIES**

311 Functional gene libraries supported the metagenomic analysis and also suggested a greater
312 genetic potential for anaerobic hydrocarbon degradation at the two sites near the DWH well,
313 with respect to the *assA* and *bssA* genes. The *assA* and *bssA* genes encode the catalytic subunits
314 of the glyoxyl radical enzymes, alkylsuccinate synthase (ASS, MAS) (Callaghan et al., 2008;
315 Grundmann et al., 2008) and benzylsuccinate synthase (BSS) (Leuthner et al., 1998),
316 respectively. Based on previous studies, ASS/MAS presumably catalyzes the addition of *n*-
317 alkanes to fumarate (Callaghan et al., 2008; Grundmann et al., 2008) to form
318 methylalkylsuccinic acids (for review see Widdel and Grundmann, 2010), whereas BSS
319 catalyzes the addition of aromatic hydrocarbons to fumarate to yield benzylsuccinic acids and
320 benzylsuccinate derivatives (for review see Boll and Heider, 2010). Both *assA* and *bssA* have
321 been used as biomarkers, in conjunction with metabolite profiling, as evidence of *in situ* aliphatic
322 and aromatic hydrocarbon degradation (Beller et al., 2008; Callaghan et al., 2010; Yagi et al.,
323 2010; Oka et al., 2011; Wawrik et al., 2012). Of the nine primer sets tested (Callaghan et al.,
324 2010), primer set 2 (specific to *bssA*) yielded four *bssA* OTUs in GoM278 sediment and four
325 *bssA* OTUs in GoM315 sediment (Figure 6). Primer set 7 (specific to *assA*) yielded eight *assA*
326 OTUs in GoM278 and eight *assA* OTUs in GoM315 (Figure 7). A comparison of the *bssA* and
327 *assA* OTU sequences revealed that there are unique and shared OTUs between the two sites.
328 Sequence identities ranged from 68.8 to 100% and 63.7 to 100% for *bssA* and *assA*, respectively.
329 Based on BlastX and BlastN, the GoM *bssA* clone sequences were similar to those from
330 uncultured bacteria as well as to *bssA* in *Thauera aromatica* K172 and *Azoarcus* sp. T
331 (Supplemental Table S2). Based on BlastX and BlastN, the GoM *assA* clone sequences were
332 similar to those from uncultured bacteria, as well as to *masD* in “*Aromatoleum*” sp. HxN1
333 (Supplemental Table S2). The *assA* and *bssA* genes were not detected in sediment collected
334 from the background site, GoM023, under the PCR conditions and primers tested in this study.

335 METABOLITE PROFILING

336 We specifically looked for the presence of alkylsuccinate derivatives that were presumed
337 metabolites formed by the addition of hydrocarbon substrates across the double bond of fumarate
338 (Biegert et al., 1996; Kropp et al., 2000; Elshahed et al., 2001; Gieg and Suflita, 2005). For
339 example, the presence of benzyl- or alkyl-succinic acids indicates the anaerobic metabolic decay
340 of alkylated aromatic or *n*-alkane hydrocarbons, respectively (Davidova et al., 2005; Duncan et
341 al., 2009; Parisi et al., 2009). Straight chain alkanes and alkenes with carbon lengths from C11 to
342 C14 and from C13 to C22, respectively, were detected using GC/MS in the two sites closest to
343 the spill site (GoM278 and GoM315). A few branched alkanes and alkenes were also observed.
344 *n*-Alkane and *n*-alkene hydrocarbons were not detected in the background sample (GoM023).
345 With GC/MS, alkanolic acids in GoM278 (2.7 km) with lengths between C14 and C18 were
346 detected, whereas the lengths ranged from C7 to C22 in GoM315 (0.5 km). Alkylsuccinate or
347 alkylmalonates metabolites typically associated with the anaerobic biodegradation of *n*-alkanes
348 via “fumarate addition” were below detection levels in all samples. However, putative
349 benzylsuccinates were identified in the samples, based on their metastable fragmentation pattern
350 of $\approx 5\%$ loss of CO₂ and no detectable loss of H₂O in MS mode. The highest abundances were
351 observed for C16 to C19 benzylsuccinates (Figure 8), and their abundances were also three times
352 higher in GoM315 (0.5 km) than in the other two samples. The presence of benzylsuccinates is
353 consistent with the detection of *bssA* genotypes. Benzoate, a central metabolite of both aerobic
354 and anaerobic hydrocarbon metabolism, was also detected in the two samples closest to the spill
355 site.

356 COMPARATIVE METAGENOMICS

357 Comparison of our metagenomic data to that of two other deep-sea metagenomes revealed a
358 number of interesting differences. The first metagenomic study examined deep subsurface
359 sediment cores (PM01*, PM01, PM50) from the nutrient-rich area of the Peru Margin (Biddle et
360 al., 2008), while the second examined an oligotrophic subsurface sediment core from the Gulf of
361 Mexico (BT Basin) prior to the DWH blowout (Biddle et al., 2011). In both studies the samples
362 were subsurface sediments collected at a depth of two meters or greater, whereas the samples
363 collected in this study were surficial samples collected at the interface between the water and the
364 sediment. Distributions of organisms at the domain level were slightly different between the
365 Peru Margin/BT Basin samples and our GoM samples, with the former harboring a greater
366 percentage of archaea (18.1-8.6% compared to 2.9-3.3%) and eukaryotes (17.7-5.8% compared
367 to 2.6-3.3%). At the phylum level, the Peru Margin and BT Basin data revealed a different
368 picture from this study with a more even distribution of Proteobacteria and Firmicutes, followed
369 by Euryarchaeota and Chloroflexi (Figure 9A). Although the functional gene patterns were
370 similar among the three studies, sequences associated with the “metabolism of aromatic
371 compounds” category were more abundant in all three of our samples (1.4-1.9%) following the
372 DWH oil-spill compared to the BT Basin (0.5%) level evaluated prior to the spill (Figure 9B).
373 Hierarchical clustering analysis, based on subsystem functional classification, revealed
374 geographical separation between the Peru Margin and Gulf of Mexico samples (Figure 10A).
375 Within the Gulf of Mexico cluster, the BT Basin clustered separately from GoM023, GoM278,
376 and GoM315. Furthermore, GoM315 and GoM278, the samples located relatively close to the
377 DWH rig, clustered separately from GoM023, the sample furthest from the DWH rig. A similar
378 pattern of separation was visualized using principal component analysis (Figure 10B) with the
379 organism classifications.

380

381 **DISCUSSION**

382 In this study, we present three new metagenomic data sets from deep-sea sediments of the Gulf
383 of Mexico following the DWH oil spill. Due to logistical and political circumstances
384 surrounding the DWH oil spill, three samples were the extent of which we were able to obtain.
385 These data, however, present a unique opportunity to examine deep-sea sediments following a
386 massive anthropogenic hydrocarbon loading event and triples the number of metagenomic
387 datasets previously available (one metagenome; Biddle et al., 2011) for deep-sea subsurface
388 sediments in the Gulf of Mexico. Although the lack of replication makes it difficult to draw
389 wide conclusions regarding the effects of hydrocarbon exposure on microbial community
390 composition and activity, these metagenomes provide important data to make baseline
391 observations that will need to be examined more thoroughly in future studies.

392
393 Two previous deep-sea metagenomic studies resulted in the suggestion that there is a core
394 metagenomic structure for deep-sea sediments, composed of four main microbial groups
395 (Euryarchaeota, Proteobacteria, Firmicutes, and Chloroflexi) that can vary depending on specific
396 parameters, such as depth, organic carbon content, and geography (Biddle et al., 2008; Biddle et
397 al., 2011). These four microbial taxa were also detected in GoM sediment samples in the present
398 work; however, they do not constitute the four major groups detected in this report
399 (Proteobacteria, Bacteroidetes, Firmicutes, and Actinobacteria). Despite similarities to the
400 microbial communities described previously (Biddle et al., 2008; Biddle et al., 2011), our cross-
401 study comparisons via hierarchical clustering and principal component analyses reveal a distinct
402 separation between the Peru Margin communities (Biddle et al., 2008) and both Gulf of Mexico
403 communities (Biddle et al., 2011, and current report). This is of particular interest, since the two
404 previous studies were subsurface samples, compared to our surficial samples. A metagenomic
405 fosmid library of deep-sea sediments from the organic-rich Qiongdongnan Basin in the South
406 China Sea (Hu et al., 2010) revealed a community structure that was more similar to this study
407 than to those of the Biddle et al. (2008; 2011) studies. These data suggest the possibility that
408 organic carbon content is more relevant to microbial community structure than geography. Hu et
409 al. (2010) detected Proteobacteria as the dominant (~43%) bacterial phylum, and
410 Deltaproteobacteria as the most abundant class within this phylum. KEGG analysis of the fosmid
411 ends also revealed genes associated with the biodegradation pathways of numerous xenobiotics
412 including, but not limited to dichloroethane, benzoate, biphenyl, ethylbenzene, fluorene,
413 naphthalene, anthracene, styrene, tetrachloroethene, and gamma-hexachlorocyclohexane. The
414 detection of genes related to the biodegradation of xenobiotic compounds in their study and ours
415 supports the premise that deep-sea sediment microbial communities have the potential to
416 metabolize a diverse array of organic compounds, including many that are found in oil.

417
418 Numerous bacterial species have evolved the ability to metabolize aliphatic (e.g. alkanes and
419 alkenes) and aromatic hydrocarbons (e.g., BTEX and PAHs), with the most rapid and complete
420 degradation achieved through aerobic processes (Fritsche and Hofrichter, 2008). The majority of
421 characterized oil-degraders within marine systems are aerobic members of the Alpha- and
422 Gammaproteobacteria (for reviews see Head et al., 2006; Kim and Kwon, 2010) that use mono-
423 and dioxygenases to initiate degradation (Haddock, 2010; Rojo, 2010). This includes
424 *Alcanivorax borkumensis*, a ubiquitous gammaproteobacterium in marine environments, which is
425 known to utilize aliphatic hydrocarbons (Yakimov et al., 1998; Schneiker et al., 2006; dos Santos
426 et al., 2010). Following the DWH blow out, *Oceanospirillales* was shown to be the dominant

427 bacterial orders associated with the resulting deepwater (~1100 m) oil plume (i.e., more than
428 90% of the sequences were classified as *Oceanospirillales*, predominantly from one
429 monophyletic lineage (Hazen et al., 2010)). Our metagenomic analysis revealed the presence,
430 in all three deep-sea sediment libraries, of bacteria belonging to the broader *Oceanospirillales*
431 order, including 51 - 61 sequences specifically recruited to the *A. borkumensis* genome in each
432 sample (Figure 4). The abundance of *Oceanospirillales*, however, was relatively low (< 2% of
433 bacterial sequences) compared to those found in the deep water oil plume (Hazen et al., 2010;
434 Mason et al., 2012). GoM315, GoM278, and GoM023 exhibited similar levels of
435 *Oceanospirillales* spp. (1.5, 1.7, and 1.4% of bacterial sequences, respectively) and
436 Gammaproteobacteria in general (19, 20, and 19% of bacterial sequences, respectively), showing
437 no correlation to the hydrocarbon levels associated with each sample. Alphaproteobacteria
438 associated with aerobic oil degradation were also found at very low abundances with similar
439 levels across the deep-sea sediment samples, including *Roseovarius* spp. and *Mauricaulis* spp. (<
440 0.5 and < 0.3% of bacterial species, respectively). Nonetheless, mono- and dioxygenases were
441 present in all three samples. These data indicate that the potential for aerobic degradation is
442 present in these samples, albeit at much lower levels than observed in the water column (Hazen
443 et al., 2010; Mason et al., 2012), and that the level of hydrocarbon exposure did not significantly
444 impact this potential. One potential explanation for this is that the hydrocarbons susceptible to
445 aerobic degradation were depleted rapidly in the water column, either by dispersants or by the
446 quick responding bacterial blooms of aerobic hydrocarbon-degrading microorganisms (Hazen et
447 al., 2010; Kessler et al., 2011). As a result, the hydrocarbon loading that occurred in the deep-sea
448 sediments may not have promoted the growth of microorganisms capable of aerobic hydrocarbon
449 degradation, but rather that of microorganisms capable of degrading the remaining recalcitrant
450 hydrocarbons that require anaerobic processing. It is also possible, however, that we sampled at
451 a time when the community was just beginning to shift to reflect the increasing importance of
452 anaerobic microbes. Future work involving time series samples and/or the analysis of aerobic
453 metabolites will be necessary to provide further insights.

454
455 Anaerobic biodegradation of hydrocarbons is an important biogeochemical process in a variety
456 of deep subsurface environments (Aitken et al., 2004; Jones et al., 2007; Wawrik et al., 2012).
457 Studies during the last two decades have highlighted the ability of anaerobic microorganisms to
458 metabolize a variety of hydrocarbons, including *n*-alkanes, *n*-alkenes, alicyclic hydrocarbons,
459 and mono- and polycyclic aromatic compounds (for reviews see Boll and Heider, 2010; Widdel
460 and Grundmann, 2010; Widdel et al., 2010). To date, the most well-characterized anaerobic
461 mechanism for hydrocarbon activation and degradation is addition to fumarate (“fumarate
462 addition”), in which the parent hydrocarbon substrate is added across the double bond of
463 fumarate via glycyl radical enzymes (for reviews see Boll and Heider, 2010; Widdel and
464 Grundmann, 2010). Deltaproteobacteria, in particular, have been implicated in “fumarate
465 addition” of both aromatic and aliphatic hydrocarbons (Widdel et al., 2010). In this study,
466 metagenomic analysis revealed an increase in the percentage of bacterial sequences that
467 represent Deltaproteobacteria associated with the sediment cores closest to the DWH well, where
468 there were higher levels of PAHs (Operational Science Advisory Team, 2010) and detectable
469 levels of alkanes and alkenes. It should be noted that the increase in Deltaproteobacteria is
470 potentially an indirect effect of the increased dead biomass from the oil spill, which cannot be
471 ruled out by this study. In any case, recruitment plots demonstrated that 857 and 547 of the
472 metagenomic sequences mapped onto the Deltaproteobacterial genomes of *Desulfatibacillum*

473 *alkenivorans* AK-01 and *Geobacter metallireducens* GS-15, respectively. The increases in
474 Deltaproteobacteria were also concurrent with an increase in functional genes involved in the
475 anaerobic degradation of hydrocarbons, such as benzylsuccinate synthase, acetyl-CoA
476 acetyltransferase and benzoyl-CoA reductase. These results suggest that the microbial response
477 to anthropogenic hydrocarbon loading may mirror aspects of microbial communities associated
478 with Gulf of Mexico natural seeps, where Deltaproteobacteria play a dominant role in their
479 biogeochemical activity, including anaerobic hydrocarbon degradation (Orcutt et al., 2010;
480 Lloyd et al., 2010). Most likely, however, the specific genus-level lineages of
481 Deltaproteobacteria will be dependent on the hydrocarbon source present, since the natural gas-
482 rich seeps contain specialized deltaproteobacterial groups for anaerobic methane utilization that
483 are unlikely to thrive in sediments with more recalcitrant oil remnants.

484
485 Clone libraries of *assA* and *bssA* supported the metagenomic analysis. Both genotypes were
486 detected in sediments near the DWH well (GoM278 and GoM315), but not at the unimpacted
487 site (GoM023). The presence of *assA* and *bssA* suggests the potential for both aliphatic and
488 aromatic hydrocarbon activation via “fumarate addition” Although *assA* genotypes were detected
489 in sediments from GoM278 and GoM315, alkylsuccinates were not detected in these samples.
490 However, this should not be interpreted as conclusive evidence that aliphatic substrates were not
491 being metabolized. The requisite metabolites are usually in low abundance (typically nM) and
492 transitory and could have easily been further metabolized or been below method detection limits.
493 The alkanolic acid compounds detected in the GoM samples could have been formed via multiple
494 biological pathways, including aerobic and anaerobic transformation of aliphatic hydrocarbons,
495 but they are not highly diagnostic. Despite the non-detection of alkylsuccinates, both *bssA*
496 genotypes *and* the putative benzylsuccinate metabolites were detected in the two sediment cores
497 closest to the spill site, suggesting *in situ* anaerobic biodegradation of alkylbenzenes. This is
498 consistent with the increased number of genes related to “aromatic metabolism” detected in the
499 corresponding sediments via metagenomic analysis. Benzoate was also detected in GoM278 and
500 GoM315 sediments, suggesting further transformation of the benzylsuccinate derivatives of
501 monoaromatic hydrocarbons (Beller and Spormann, 1997; Leuthner et al., 1998). However,
502 benzoate can be formed during the metabolism of a wide variety of aromatic compounds under
503 aerobic *and* anaerobic conditions.

504
505 Overall, this study took an interdisciplinary approach of investigating the phylogenetic
506 composition and functional potential of Gulf of Mexico deep-sea sediment communities
507 following the Deepwater Horizon oil spill. Based on metagenomic analyses, functional gene
508 clone libraries, and metabolite profiling, the data herein suggest that the presence of PAHs,
509 alkanes, and alkenes may influence the microbial community through the enrichment of
510 Deltaproteobacteria capable of anaerobic hydrocarbon metabolism. This evidence suggests that
511 the microbial communities exposed to anthropogenic hydrocarbon loading in the Gulf of
512 Mexico deep-sea sediments likely impacted the bioremediation of the Deepwater Horizon oil
513 spill through anaerobic degradation, which has been previously overlooked. The integrated
514 approach used herein augments other efforts to deduce the fate of the oil spilled in the DWH
515 incident and to assess the impact of the spill on the indigenous microbial communities.

516 517 **ACKNOWLEDGEMENTS**

518 We would like to thank the following individuals at LBNL that were instrumental in collecting,

519 preserving and aseptically sectioning the deep-sea sediment cores: Sharon Borglin, Yvette
520 Piceno, Dominique Joyner, Janet Jansson, and Olivia Mason. We would also like to thank
521 Andreas Teske for his thoughtful comments and critical review of the manuscript. This study
522 was supported by the National Science Foundation (MCB-1049411) and (MCB-1049409) to
523 PJM and JMS, respectively, by the program SPP 1319 of the Deutsche Forschungsgemeinschaft
524 (grant to BTG in support of MD), and also in part by an NSF grant (MCB-0921265) to AVC.
525 BTG and MD also thank the EPSRC Mass Spectrometry Service at the University of Wales
526 (Swansea) for mass spectrometric analyses.
527
528

529 **REFERENCES**

- 530 Aitken, C.M., Jones, D.M., and Larter, S.R. (2004). Anaerobic hydrocarbon biodegradation in
531 deep subsurface oil reservoirs. *Nature* 431.
- 532 Aktas, D.F., Lee, J.S., Little, B.J., Ray, R.I., Davidova, I.A., Lyles, C.N., Suflita, J.M. (2010).
533 Anaerobic Metabolism of Biodiesel and Its Impact on Metal Corrosion. *Energ. Fuels* 24,
534 2924-2928.
- 535 Atlas, R.M. (1981). Microbial degradation of petroleum hydrocarbons: an environmental
536 perspective. *Microbiol. Rev.* 45, 180.
- 537 Beller, H.R., and Spormann, A.M. (1997). Anaerobic activation of toluene and o-xylene by
538 addition to fumarate in denitrifying strain T. *J. Bacteriol.* 179, 670-676.
- 539 Beller, H.R., Kane, S.R., Legler, T.C., McKelvie, J.R., Lollar, B.S., Pearson, F., Balsler, L.,
540 Mackay, D.M. (2008). Comparative assessments of benzene, toluene, and xylene natural
541 attenuation by quantitative polymerase chain reaction analysis of a catabolic gene,
542 signature metabolites, and compound-specific isotope analysis. *Environ. Sci. Technol.* 42,
543 6065-6072.
- 544 Biddle, J.F., Fitz-Gibbon, S., Schuster, S.C., Brenchley, J.E., and House, C.H. (2008).
545 Metagenomic signatures of the Peru Margin seafloor biosphere show a genetically
546 distinct environment. *Proc. Natl. Acad. Sci. USA* 105, 10583-10588.
- 547 Biddle, J.F., White, J.R., Teske, A.P., and House, C.H. (2011). Metagenomics of the subsurface
548 Brazos-Trinity Basin (IODP site 1320): comparison with other sediment and
549 pyrosequenced metagenomes. *ISME J.* 5, 1038-1046.
- 550 Biegert, T., Fuchs, G., and Heider, J. (1996). Evidence that anaerobic oxidation of toluene in the
551 denitrifying bacterium *Thauera aromatica* is initiated by formation of benzylsuccinate
552 from toluene and fumarate. *Euro. J. Biochem.* 238, 661-668.
- 553 Boll, M., and Heider, J. (2010). "Anaerobic degradation of hydrocarbons: mechanisms of C-H
554 bond activation in the absence of oxygen," in *Handbook of Hydrocarbon and Lipid
555 Microbiology*, eds. K. Timmis, T. Mcgenity, J. Van Der Meer & V. De Lorenzo. (Berlin
556 Heidelberg: Springer-Verlag), 1011-1024.
- 557 Callaghan, A.V., Davidova, I.A., Savage-Ashlock, K., Parisi, V.A., Gieg, L.M., Suflita, J.M.,
558 Kukor, J.J., and Wawrik, B. (2010). Diversity of benzyl- and alkylsuccinate synthase
559 genes in hydrocarbon-impacted environments and enrichment cultures. *Environ. Sci.
560 Tech.* 44, 7287-7294.
- 561 Callaghan, A.V., Morris, B.E.L., Pereira, I.A.C., McInerney, M.J., Austin, R.N., Groves, J.T.,
562 Kukor, J.J., Suflita, J.M., Young, L.Y., Zylstra, G.J., and Wawrik, B. (2012). The genome
563 sequence of *Desulfatibacillum alkenivorans* AK-01: a blueprint for anaerobic alkane
564 oxidation. *Environ. Microbiol.* 14, 101-113.
- 565 Callaghan, A.V., Wawrik, B., Ní Chadhain, S.M., Young, L.Y., and Zylstra, G.J. (2008).
566 Anaerobic alkane-degrading strain AK-01 contains two alkylsuccinate synthase genes.
567 *Biochem. Biophys. Res. Commun.* 366, 142-148.
- 568 Colwell, R.K. (2006). EstimateS: statistical estimation of species richness and shared species for
569 samples. Version 8. Persistent URL, <purl.oclc.org/estimates>.
- 570 D'hondt, S., Jørgensen, B.B., Miller, D.J., Batzke, A., Blake, R., Cragg, B.A., Cypionka, H.,
571 Dickens, G.R., Ferdelman, T., Hinrichs, K.-U., Holm, N.G., Mitterer, R., Spivack, A.,
572 Wang, G., Bekins, B., Engelen, B., Ford, K., Gettemy, G., Rutherford, S.D., Sass, H.,
573 Skilbeck, C.G., Aiello, I.W., Guèrin, G., House, C.H., Inagaki, F., Meister, P., Naehr, T.,
574 Niitsuma, S., Parkes, R.J., Schippers, A., Smith, D.C., Teske, A., Wiegel, J., Padilla,

575 C.N., and Acosta, J.L.S. (2004). Distributions of microbial activities in deep subseafloor
576 sediments. *Science* 306, 2216-2221.

577 D'Hondt, S., Spivack, A.J., Pockalny, R., Ferdelman, T.G., Fischer, J.P., Kallmeyer, J., Abrams,
578 L.J., Smith, D.C., Graham, D., Hasiuk, F., Schrum, H., Stancin, A.M. (2009). Subseafloor
579 sedimentary life in the South Pacific Gyre. *Proc. Natl. Acad. Sci. U S A* 106, 11651-
580 11656. Davidova, I.A., Gieg, L.M., Nanny, M., Kropp, K.G., and Suflita, J.M. (2005).
581 Stable isotopic studies of n-alkane metabolism by a sulfate-reducing bacterial enrichment
582 culture. *Appl. Environ. Microbiol.* 71, 8174-8182.

583 Dos Santos, V., Sabirova, J., Timmis, K., Yakimov, M., and Golyshin, P. (2010). "*Alcanivorax*
584 *borkumensis*," in *Handbook of Hydrocarbon and Lipid Microbiology*, eds. K. Timmis, T.
585 Mcgenity, J. Van Der Meer & V. De Lorenzo. (Berlin Heidelberg: Springer-Verlag),
586 1011-1024.

587 Duncan, K.E., Gieg, L.M., Parisi, V.A., Tanner, R.S., Tringe, S.G., Bristow, J., and Suflita, J.M.
588 (2009). Biocorrosive thermophilic microbial communities in Alaskan North Slope oil
589 facilities. *Environn Sci. Tech.* 43, 7977-7984.

590 Eglund, P.G., Pelletier, D.A., Dispensa, M., Gibson, J., and Harwood, C.S. (1997). A cluster of
591 bacterial genes for anaerobic benzene ring biodegradation. *Proc. Nat. Acad. Sci. USA* 94,
592 6484-6489.

593 Elshahed, M.S., Gieg, L.M., McInerney, M.J., and Suflita, J.M. (2001). Signature metabolites
594 attesting to the in situ attenuation of alkylbenzenes in anaerobic environments. *Environn*
595 *Sci. Tech.* 35, 682-689.

596 Fritsche, W., and Hofrichter (2008). "Aerobic degradation by microorganisms," in
597 *Biotechnology: environmental processes II, Volume 11b, Second Edition*, eds. H.J. Rehm
598 & G. Reed. (Weinheim, Germany: Wiley-VCH Verlag GmbH), 146-164.

599 Gieg, L.M. and Suflita, J.M. (2005). "Metabolic indicators of anaerobic hydrocarbon
600 biodegradation in petroleum-laden environments," in *Petroleum Microbiology*, eds. B.
601 Ollivier & M. Magot. (Washington, DC: ASM Press), 356-371.

602 Grundmann, O., Behrends, A., Rabus, R., Amann, J., Halder, T., Heider, J., and Widdel, F.
603 (2008). Genes encoding the candidate enzyme for anaerobic activation of n-alkanes in the
604 denitrifying bacterium, strain HxN1. *Environ. Microbiol.* 10, 376-385.

605 Haddock, J.D. (2010). "Aerobic degradation of aromatic hydrocarbons: enzyme structures and
606 catalytic mechanisms," in *Handbook of Hydrocarbon and Lipid Microbiology*, eds. K.
607 Timmis, T. Mcgenity, J. Van Der Meer & V. De Lorenzo. (Berlin Heidelberg: Springer-
608 Verlag), 1057-1069.

609 Hazen, T.C., Dubinsky, E.A., Desantis, T.Z., Andersen, G.L., Piceno, Y.M., Singh, N., Jansson,
610 J.K., Probst, A., Borglin, S.E., Fortney, J.L., Stringfellow, W.T., Bill, M., Conrad, M.E.,
611 Tom, L.M., Chavarria, K.L., Alusi, T.R., Lamendella, R., Joyner, D.C., Spier, C.,
612 Baelum, J., Auer, M., Zelma, M.L., Chakraborty, R., Sonnenthal, E.L., D'haeseleer, P.,
613 Holman, H.N., Osman, S., Lu, Z., Van Nostrand, Deng, Y., Zhou, J., and Mason, O.U.
614 (2010). Deep-sea oil plume enriches indigenous oil-degrading bacteria. *Science* 330, 204-
615 208.

616 Head, I.M., Jones, D.M., and Rölting, W.F.M. (2006). Marine microorganisms make a meal of
617 oil. *Nat. Rev. Microbiol.* 4, 173-182.

618 Hu, Y., Fu, C., Yin, Y., Cheng, G., Lei, F., Yang, X., Li, J., Ashforth, E.J., Zhang, L., and Zhu,
619 B. (2010). Construction and preliminary analysis of a deep-sea sediment metagenomic

620 fosmid library from Qiongdongnan Basin, South China Sea. *Mar. Biotechnol.* 12, 719-
621 727.

622 Jernelov, A., and Linden, O. (1981). Ixtoc I: a case study of the world's largest oil spill. *Ambio*
623 10, 299-306.

624 Jones, D., Head, I., Gray, N., Adams, J., Rowan, A., Aitken, C., Bennett, B., Huang, H., Brown,
625 A., and Bowler, B. (2007). Crude-oil biodegradation via methanogenesis in subsurface
626 petroleum reservoirs. *Nature* 451, 176-180.

627 Jørgensen, B.B. (2011). Deep seafloor microbial cells on physiological standby. *Proc Natl*
628 *Acad Sci USA* 108, 18193-18194.

629 Joye, S.B., Boetius, A., Orcutt, B.N., Montoya, J.P., Schulz, H.N., Erickson, M.J., Lugo, S.K..
630 (2004). The anaerobic oxidation of methane and sulfate reduction in sediments from Gulf
631 of Mexico cold seeps. *Chem. Geol.* 205, 219-238.

632 Kallmeyer, J., Pockalny, R., Adhikari, R.R., Smith, D.C., D'Hondt, S.. 2012. Global distribution
633 of microbial abundance and biomass in subseafloor sediment. *Proc Natl Acad Sci USA*
634 10.1073/pnas.1203849109.

635 Kennedy, J., Marchesi, J.R., and Dobson, A.D.W. (2008). Marine metagenomics: strategies for
636 the discovery of novel enzymes with biotechnological applications from marine
637 environments. *Microb. Cell. Fact* 7, 27.

638 Kessler, J.D., Valentine, D.L., Redmond, M.C., Du, M., Chan, E.W., Mendes, S.D., Quiroz,
639 E.W., Villanueva, C.J., Shusta, S.S., Werra, L.M., Yvon-Lewis, S.A., and Weber, T.C.
640 (2011). A persistent oxygen anomaly reveals the fate of spilled methane in the deep Gulf
641 of Mexico. *Science* 331, 312-315.

642 Kim, S., and Kwon, K. (2010). "Marine, hydrocarbon-degrading Alphaproteobacteria," in
643 *Handbook of Hydrocarbon and Lipid Microbiology*, eds. K. Timmis, T. Mcgenity, J. Van
644 Der Meer & V. De Lorenzo. (Berlin Heidelberg: Springer-Verlag), 1707-1714.

645 Kropp, K.G., Davidova, I.A., and Suflita, J.M. (2000). Anaerobic oxidation of n-dodecane by an
646 addition reaction in a sulfate-reducing bacterial enrichment culture. *Appl. Environ.*
647 *Microbiol.* 66, 5393-5398.

648 Kumar, S., Nei, M., Dudley, J., and Tamura, K. (2008). MEGA: a biologist-centric software for
649 evolutionary analysis of DNA and protein sequences. *Brief. Bioinform.* 9, 299-306.

650 Leuthner, B., Leutwein, C., Schulz, H., Hörth, P., Haehnel, W., Schiltz, E., Schagger, H., and
651 Heider, J. (1998). Biochemical and genetical characterization of benzylsuccinate synthase
652 from *Thauera aromatica*: a new glyceryl radical enzyme catalyzing the first step in
653 anaerobic toluene metabolism. *Mol. Microbiol.* 28, 615-628.

654 Lloyd, K.G., Lapham, L., Teske, A. (2006). An anaerobic methane-oxidizing community of
655 ANME-1b archaea in hypersaline Gulf of Mexico sediments. *Appl. Environ. Microbiol.*
656 72, 7218-7230.

657 Lloyd, K.G., Albert, D.B., Biddle, J.F., Chanton, J.P., Pizarro, O., Teske, A. (2010). Spatial
658 structure and activity of sedimentary microbial communities underlying a *Beggiatoa* spp.
659 mat in a Gulf of Mexico hydrocarbon seep. *PLoS One* 5, e8738.

660 Lovley, D.R., Giovannoni, S.J., White, D.C., Champine, J.E., Phillips, E.J.P., Gorby, Y.A., and
661 Goodwin, S. (1993). *Geobacter metallireducens* gen. nov. sp. nov., a microorganism
662 capable of coupling the complete oxidation of organic compounds to the reduction of iron
663 and other metals. *Archives Microbiol.* 159, 336-344.

664 Mason, O.U., Hazen, T.C., Borglin, S., Chain, P.S.G., Dubinsky, E.A., Fortney, J.L., Han, J.,
665 Holman, H.-Y.N., Hultman, J., Lamendella, R., Mackelprang, R., Malfatti, S., Tom,

666 L.M., Tringe, S.G., Woyke, T., Zhou, J., Rubin, E.M., and Jansson, J.K. (2012).
667 Metagenome, metatranscriptome and single-cell sequencing reveal microbial response to
668 Deepwater Horizon oil spill. *ISME J.* 6, 1715-1727.

669 Meyer, F., Paarmann, D., D'souza, M., Olson, R., Glass, E.M., Kubal, M., Paczian, T.,
670 Rodriguez, A., Stevens, R., Wilke, A., Wilkening, J., and Edwards, R.A. (2008). The
671 metagenomics RAST server – a public resource for the automatic phylogenetic and
672 functional analysis of metagenomes. *BMC Bioinform.* 9, 386-394.

673 Muyzer, G., De Waal, E.C., and Uitterlinden, A.G. (1993). Profiling of complex microbial
674 populations by denaturing gradient gel electrophoresis analysis of polymerase chain
675 reaction-amplified genes coding for 16S rRNA. *Appl. Environ. Microbiol.* 59, 695-700.

676 Oka, A.R., Phelps, C.D., Zhu, X., Saber, D.L., and Young, L. (2011). Dual biomarkers of
677 anaerobic hydrocarbon degradation in historically contaminated groundwater. *Environ.*
678 *Sci. Technol.* 45, 3407-3414.

679 Operational Science Advisory Team (2010). Summary report for sub-sea and sub-surface oil and
680 dispersant detection: sampling and monitoring. December 17, 2010.

681 Orcutt, B.N., Joye, S.B., Kleindienst, S., Knittel, K., Ramette, A., Reitz, A., Samarkin, V.,
682 Treude, T., Boetius, A.. (2010). Impact of natural oil and higher hydrocarbons on
683 microbial diversity, distribution, and activity in Gulf of Mexico cold-seep sediments.
684 *Deep Sea Research Part II: Topical Studies in Oceanography* 57, 2008-2021. Parisi, V.A.,
685 Brubaker, G.R., Zenker, M.J., Prince, R.C., Gieg, L.M., Da Silva, M.L.B., Alvarez, P.J.J.,
686 and Suflita, J.M. (2009). Field metabolomics and laboratory assessments of anaerobic
687 intrinsic bioremediation of hydrocarbons at a petroleum-contaminated site. *Micro.*
688 *Biotechnol.* 2, 202-212.

689 Ramseur, J.L. (2010). "Deepwater Horizon oil spill: the fate of the oil". Congressional Research
690 Service.

691 Rojo, F. (2010). "Enzymes for aerobic degradation of alkanes," in *Handbook of Hydrocarbon*
692 *and Lipid Microbiology*, eds. K. Timmis, T. Mcgenity, J. Van Der Meer & V. De
693 Lorenzo. (Berlin Heidelberg: Springer-Verlag), 781-797.

694 Schneiker, S., Martins Dos Santos, V., Bartels, D., Bekel, T., Brecht, M., Buhrmester, J.,
695 Chernikova, T.N., and Denaro, R. (2006). Genome sequence of the ubiquitous
696 hydrocarbon-degrading marine bacterium *Alcanivorax borkumensis*. *Nat. Biotechnol.* 24,
697 997-1004.

698 Seth-Smith, H. (2010). 'Slick' operations. *Nat. Rev. Microbiol.* 8, 538.

699 So, C.M., and Young, L. (1999). Isolation and characterization of a sulfate-reducing bacterium
700 that anaerobically degrades alkanes. *Appl. Environ. Microbiol.* 65, 2969-2976.

701 Wawrik, B., Mendivelso, M., Parisi, V.A., Suflita, J.M., Davidova, I.A., Marks, C.R., Van
702 Nostrand, J.D., Liang, Y., Zhou, J., and Huizinga, B.J. (2012). Field and laboratory
703 studies on the bioconversion of coal to methane in the San Juan Basin. *FEMS Microbiol.*
704 *Ecol.* 81, 26-42.

705 Whitman, W.B., Coleman, D.C., and Wiebe, W.J. (1998). Prokaryotes: the unseen majority.
706 *Proceed. Nat. Acad. Sci. USA* 95, 6578-6583.

707 Widdel, F., and Grundmann, O. (2010). "Biochemistry of the anaerobic degradation of non-
708 methane alkanes," in *Handbook of Hydrocarbon and Lipid Microbiology*, eds. K.
709 Timmis, T. Mcgenity, J. Van Der Meer & V. De Lorenzo. (Berlin Heidelberg: Springer-
710 Verlag), 909-924.

711 Widdel, F., Knittel, K., and Galushko, A. (2010). "Anaerobic hydrocarbon-degrading
712 microorganisms: an overview," in *Handbook of Hydrocarbon and Lipid Microbiology*,
713 eds. K. Timmis, T. Mcgenity, J. Van Der Meer & V. De Lorenzo. (Berlin Heidelberg:
714 Springer-Verlag), 1997-2021.
715 Yagi, J.M., Suflita, J.M., Gieg, L.M., DeRito, C.M., Jeon, C.O., Madsen, E.L. (2010).
716 Subsurface cycling of nitrogen and anaerobic aromatic hydrocarbon biodegradation
717 revealed by nucleic acid and metabolic biomarkers. *Appl. Environ. Microbiol.* 76, 3124-
718 3134.
719 Yakimov, M.M., Golyshin, P.N., Lang, S., Moore, E.R.B., Abraham, W.R., Lünsdorf, H., and
720 Timmis, K.N. (1998). *Alcanivorax borkumensis* gen. nov., sp. nov., a new, hydrocarbon-
721 degrading and surfactant-producing marine bacterium. *Int. J. Syst. Bacteriol.* 48, 339-
722 348.

724 **FIGURE LEGENDS**

725 **FIGURE 1.** Map of the Gulf of Mexico sampling sites. Open square – DWH rig; Filled circle –
726 sampling sites from the current study; Open circle – BT Basin sampling site from Biddle et al.
727 2011. The Peru Margin (PM) sampling sites used for comparison are described in Biddle et al.
728 (2008).

729
730 **FIGURE 2.** Phylum-level organism classifications reveal differences among the three
731 metagenomes sequenced in this study. (A) Archaea; (B) Bacteria; and (C) Eukaryotes

732
733 **FIGURE 3.** Differences are observed among the sites closest to the DWH rig and the site
734 located over a 100 km away when examining more of the Proteobacteria. (A) Proteobacteria
735 classes associated with each of the three sites reveals a decrease in the Deltaproteobacteria at the
736 far site GoM023; (B) Proteobacteria order-level classifications identify Desulfobacterales,
737 Desulfovibrioales, and Desulfomonales as the major contributors to the difference observed.

738
739 **FIGURE 4.** Recruitment plots reveal an increased association with anaerobic hydrocarbon
740 degraders in the deep sea sediments near the DWH rig. The blue circle represents the bacterial
741 contigs for the genome of interest; while the two black rings map genes on the forward and
742 reverse strands. The inner graph consists of two stacked bar plots representing the number of
743 matches to genes on the forward and reverse strands. The bars are color coded according to the
744 e-value of the matches with red (<1e-30), orange (1e-30 to 1e-20), yellow (1e-20 to 1e-10), and
745 green (1e-10 to 1e-5).

746
747 **FIGURE 5.** Functional classifications of the metagenomic sequences. (A) Similar functional
748 fingerprints are observed at the broadest subsystem classification. (B) Functional genes
749 associated with the “metabolism of aromatic compounds” reveal a decreased association with
750 “anaerobic degradation in aromatic compounds” in GoM023.

751
752 **FIGURE 6.** Neighbor-joining dendrogram of *bssA* clone sequences obtained from GoM
753 sediments (GoM278 – red; GoM315 – blue) compared to *bssA* sequences of reference strains and
754 BLAST matches. The tree was constructed using the Tajima-Nei distance method (scale bar),
755 with pairwise deletion and performing 10,000 bootstrap replicates. Bootstrap values below 65 are
756 not shown. Pyruvate formate lyase (*pfl*) served as the outgroup. Numbers in parentheses

757 represent NCBI GenBank accession numbers. Abbreviations: *bss* (benzylsuccinate synthase), *tut*
758 (“toluene-utilizing”; i.e. benzylsuccinate synthase), and *nms* (naphthylmethylsuccinate synthase).

759
760 **FIGURE 7.** Neighbor-joining dendrogram of *assA* clone sequences obtained from GoM
761 sediments (GoM278 – red; GoM315 – blue) compared to *assA/masD* sequences of reference
762 strains and BLAST matches. The tree was constructed using the Tajima-Nei distance method
763 (scale bar), with pairwise deletion and performing 10,000 bootstrap replicates. Bootstrap values
764 below 65 are not shown. Pyruvate formate lyase (*pfl*) served as the outgroup. Numbers in
765 parentheses represent NCBI GenBank accession numbers. Abbreviations: *ass* (alkylsuccinate
766 synthase); and *mas* (methylalkylsuccinate synthase).

767
768 **FIGURE 8.** Logarithm of abundance of benzyl succinates in the sample GoM315.

769
770 **FIGURE 9.** Phylogenetic and functional comparison of deep-sea sediment metagenomes across
771 three studies. (A) Phylogenetic comparison at the phylum level reveals differences among this
772 study and the two previously performed by Biddle et al. (2008, 2011). (B) Functional
773 comparison of the broadest level of subsystem classifications reveals a more similar pattern
774 between the three studies. *, denotes the “aromatic compound metabolism” category; GoM
775 combined, represents the collective data from GoM315, GoM278, and GoM023; PM combined,
776 represents the collective data from PM01*, PM01, and PM50

777
778 **FIGURE 10.** Cross-study comparisons of deep-sea metagenomes. (A) Principal component
779 analysis using organism classifications (species-level) from the current study as well as those
780 from two studies (Biddle et al., 2008, 2011) reveals clear geographic separation, in addition to a
781 second component of separation that is currently unknown. (B) Hierarchical clustering combined
782 with heat mapping based on subsystem classifications reveals similar partitioning among the
783 three studies compared.

784
785

786 **TABLES**

787 Table 1. Data from the three GoM metagenomic libraries described in this study.

788

Features	GoM315	GoM278	GoM023
Distance from Deepwater Horizon blowout	0.5 km	2.7 km	127.9 km
Depth below sea-level	1464 m	1500 m	1614 m
Basepairs sequenced prior to QC	68.7 Mb	60.7 Mb	62.2 Mb
Individual reads prior to QC	144,700	127,356	122,703
Average length of reads prior to QC	474 bp	476 bp	506 bp
Basepairs sequenced post QC	43.9 Mb	38.8 Mb	41.1 Mb
Individual reads post QC	91,717	80,841	79,524
Average length of reads post QC	478 bp	479 bp	517 bp
Prokaryotes	72,845	64,997	70,415
Eukaryotes	2056	1750	2376
Viruses	268	372	74
Functional classifications (Subsystems database)	59,175	52,599	55,130
Alpha diversity (Species-level analysis)	1003.4	981.6	908.7
Chao 1 estimate \pm s.d. (Genus-level analysis)	593 \pm 6.4	562 \pm 2.6	582 \pm 4.6
Shannon index (Genus-level analysis)	5.64	5.55	5.55

789

790

791 Table 2. Top ranked recruitment results for each of the GoM deep-sea sediment metagenomic
 792 libraries.
 793

	Recruited Genome	Rank	# of Seq	# of Features	Features in Genome	Genome Coverage (%)
GoM315	<i>Desulfobacterium autotrophicum</i> HRM2	1	464	428	4943	8.66
	'Candidatus' <i>Solibacter usitatus</i> Ellin6076	2	397	300	7826	3.83
	<i>Desulfatibacillum alkenivorans</i> AK-01	3	334	288	5252	5.48
	<i>Nitrosopumilus maritimus</i> SCM1	4	268	223	1796	12.42
	<i>Desulfococcus oleovorans</i> Hxd3	5	256	227	3265	6.95
	<i>Rhodopirellula baltica</i> SH 1	7	211	193	7325	2.63
	<i>Desulfotalea psychrophila</i> LSv54	12	185	169	3234	5.23
	<i>Haliangium ochraceum</i> DSM14365	15	174	155	6719	2.31
	<i>Cenarchaeum symbiosium</i> A	34	122	111	2017	5.5
<i>Archaeoglobus fulgidus</i> DSM4304	>300	20	18	2420	0.74	
GoM278	<i>Desulfobacterium autotrophicum</i> HRM2	1	746	593	4943	12
	<i>Desulfatibacillum alkenivorans</i> AK-01	2	426	362	5252	6.89
	<i>Nitrosopumilus maritimus</i> SCM1	3	358	294	1796	16.37
	<i>Desulfococcus oleovorans</i> Hxd3	4	332	288	3265	8.82
	<i>Desulfotalea psychrophila</i> LSv54	5	256	221	3234	6.83
	'Candidatus' <i>Solibacter usitatus</i> Ellin6076	7	218	189	7826	2.42
	<i>Cenarchaeum symbiosium</i> A	10	187	165	2017	8.18
	<i>Haliangium ochraceum</i> DSM14365	20	134	123	6719	1.83
	<i>Rhodopirellula baltica</i> SH 1	22	124	124	7325	1.69
<i>Archaeoglobus fulgidus</i> DSM4304	>300	33	31	2420	1.28	
GoM023	<i>Nitrosopumilus maritimus</i> SCM1	1	713	520	1796	28.95
	'Candidatus' <i>Solibacter usitatus</i> Ellin6076	2	564	410	7826	5.24
	<i>Cenarchaeum symbiosium</i> A	3	373	296	2017	14.68
	<i>Haliangium ochraceum</i> DSM14365	4	290	242	6719	3.6
	<i>Rhodopirellula baltica</i> SH 1	5	279	243	7325	3.32
	<i>Desulfatibacillum alkenivorans</i> AK-01	58	97	81	5252	1.54
	<i>Desulfococcus oleovorans</i> Hxd3	79	81	74	3265	2.27
	<i>Desulfobacterium autotrophicum</i> HRM2	102	72	70	4943	1.42
	<i>Desulfotalea psychrophila</i> LSv54	>200	39	37	3234	1.14
<i>Archaeoglobus fulgidus</i> DSM4304	>300	16	14	2420	0.58	

794
 795
 796
 797

Figure 1.JPEG

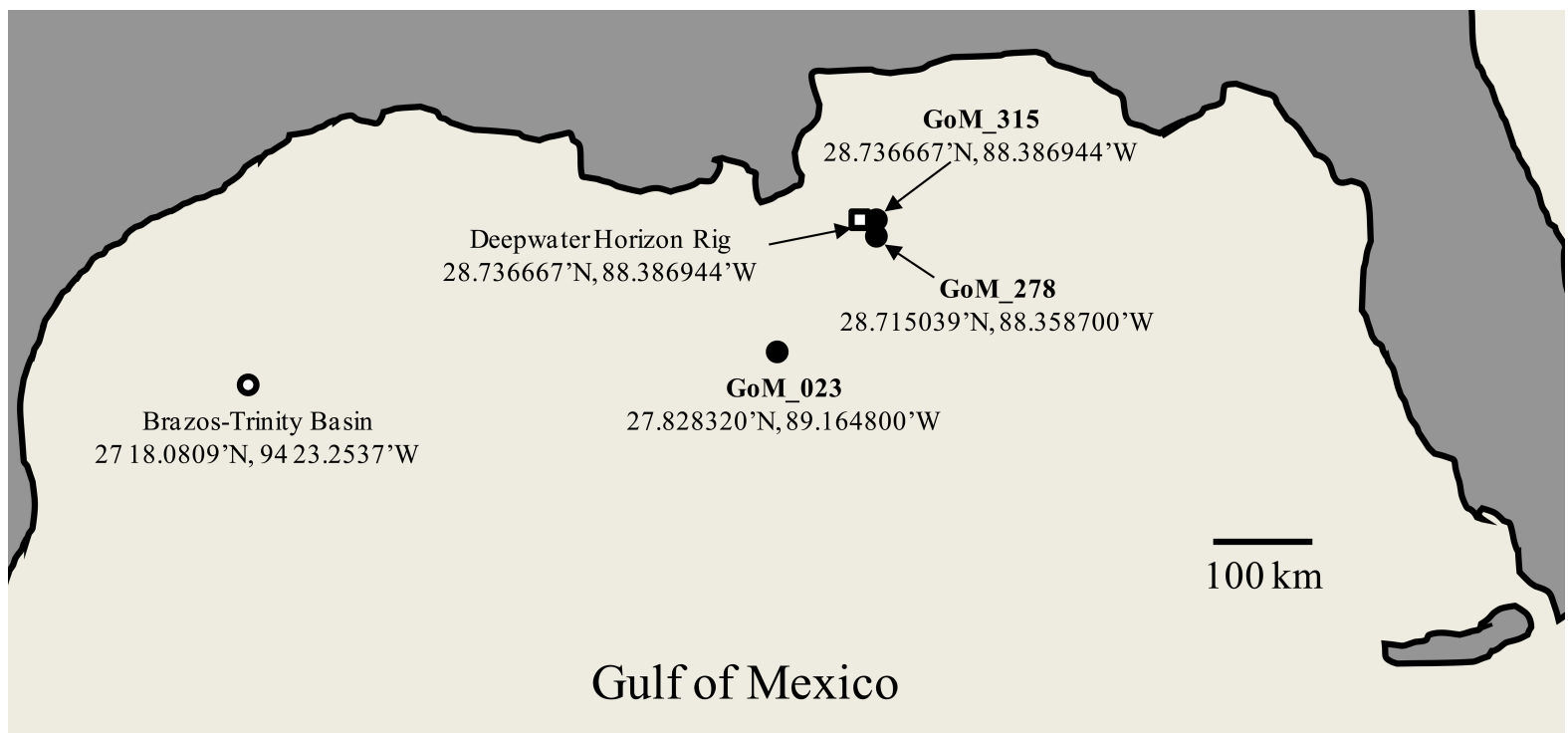
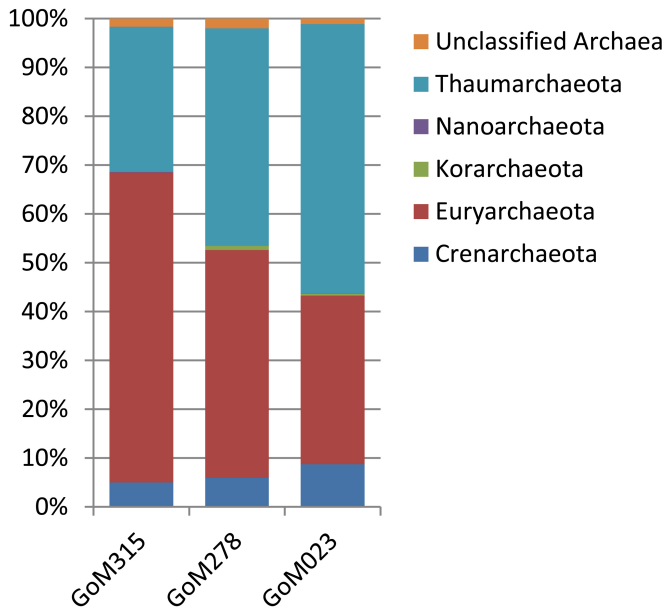
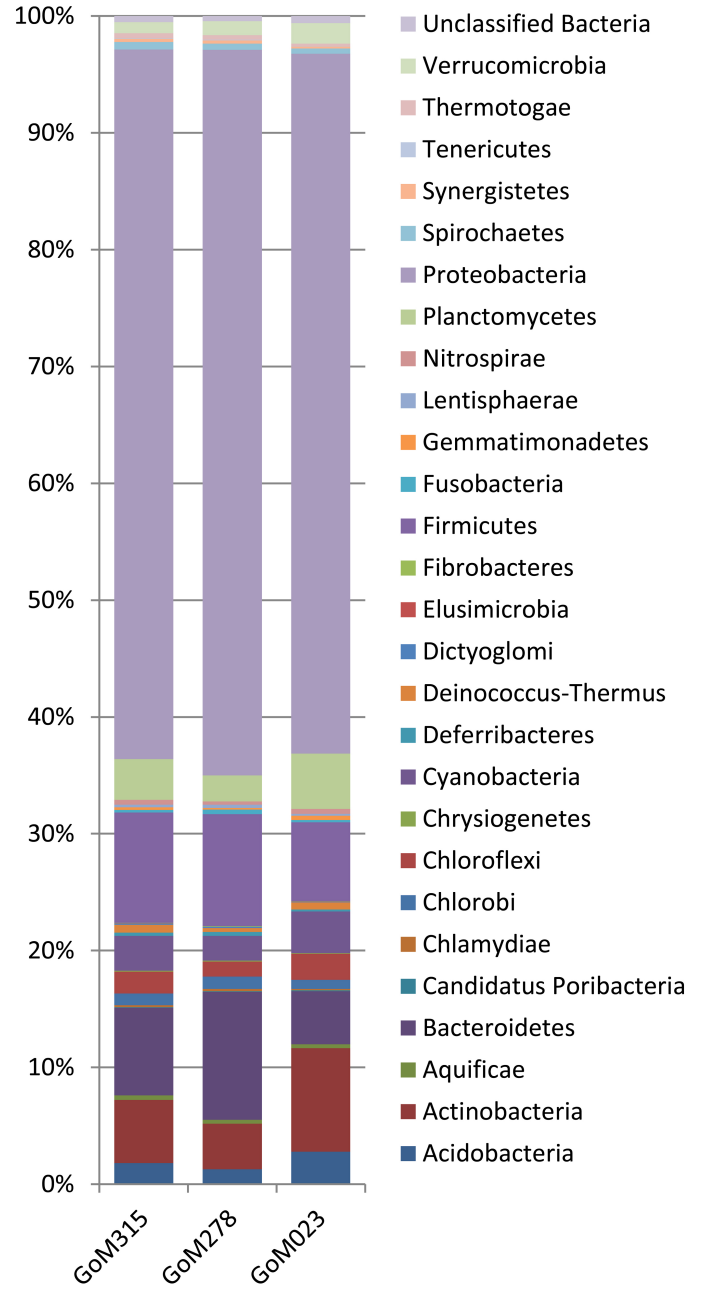


Figure 2.JPEG

A



B



C

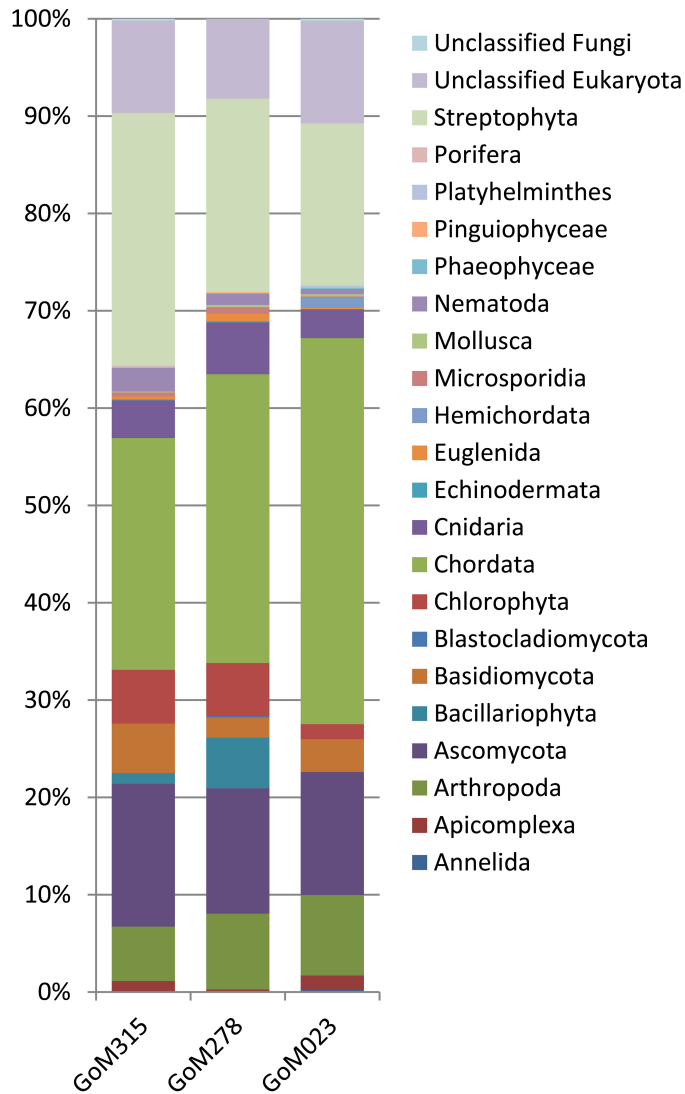
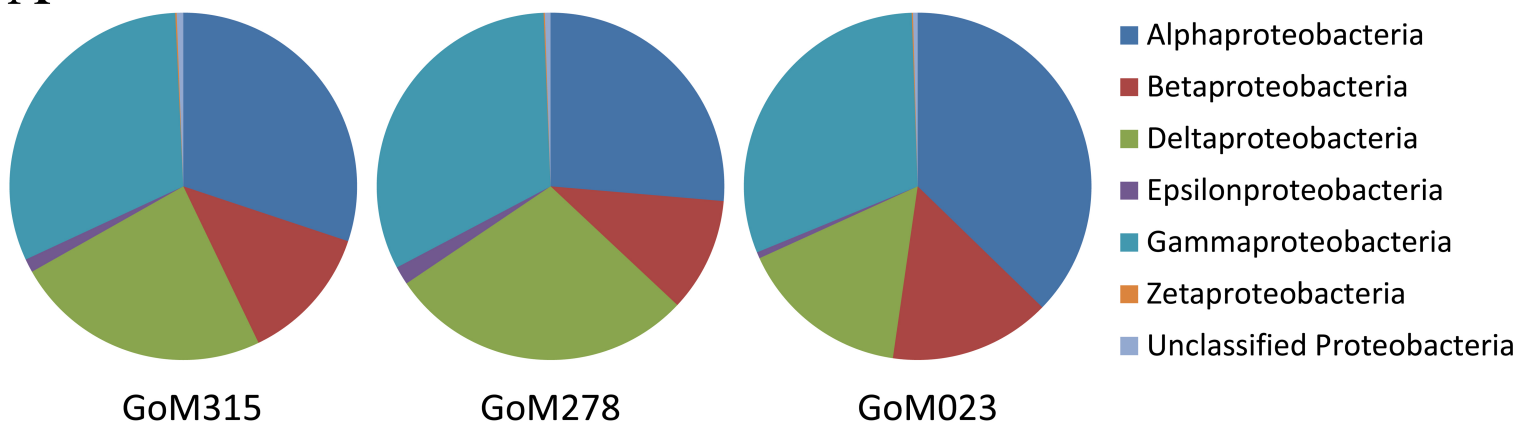


Figure 3.JPEG

A



B

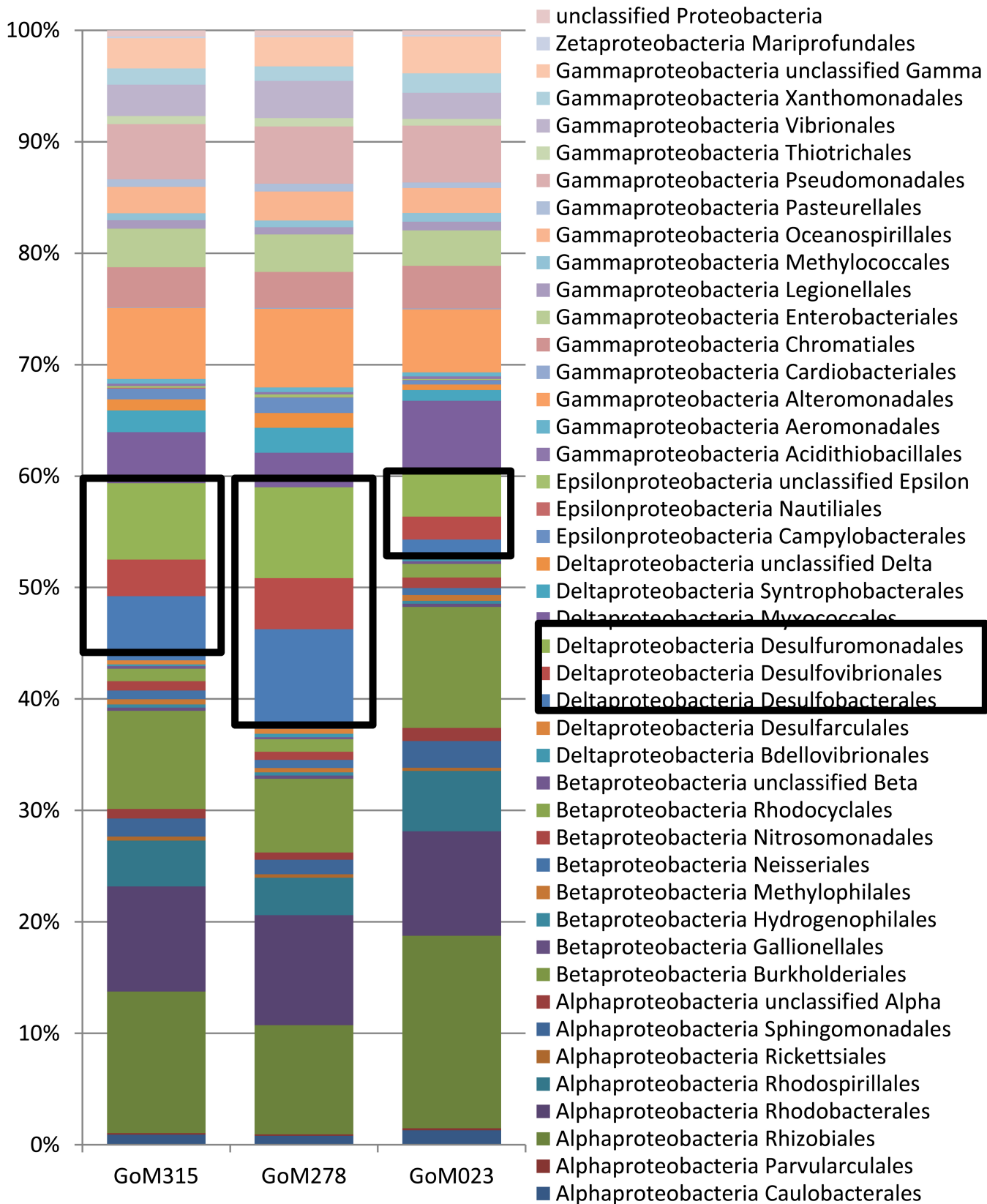
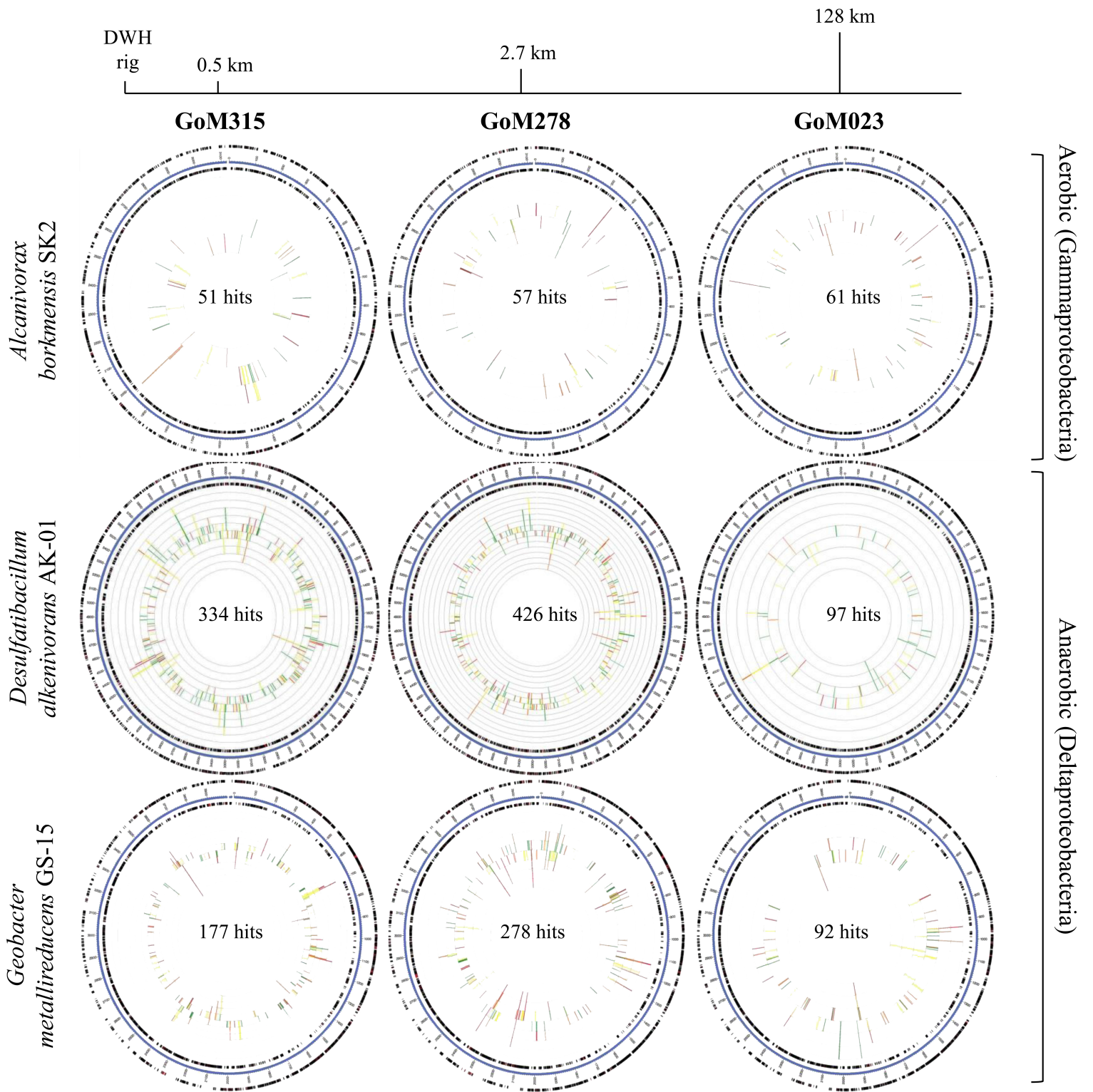
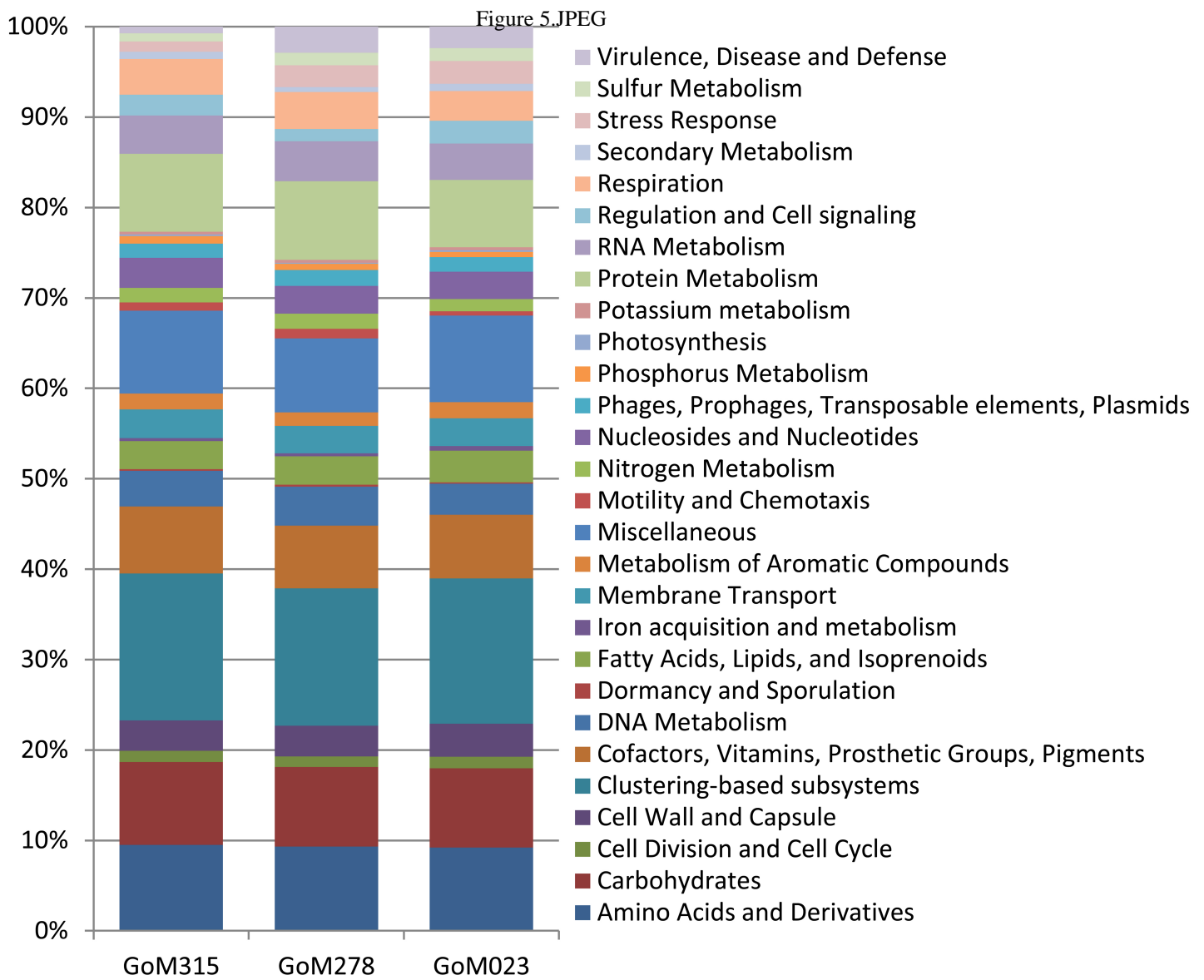


Figure 4.JPEG



A



B

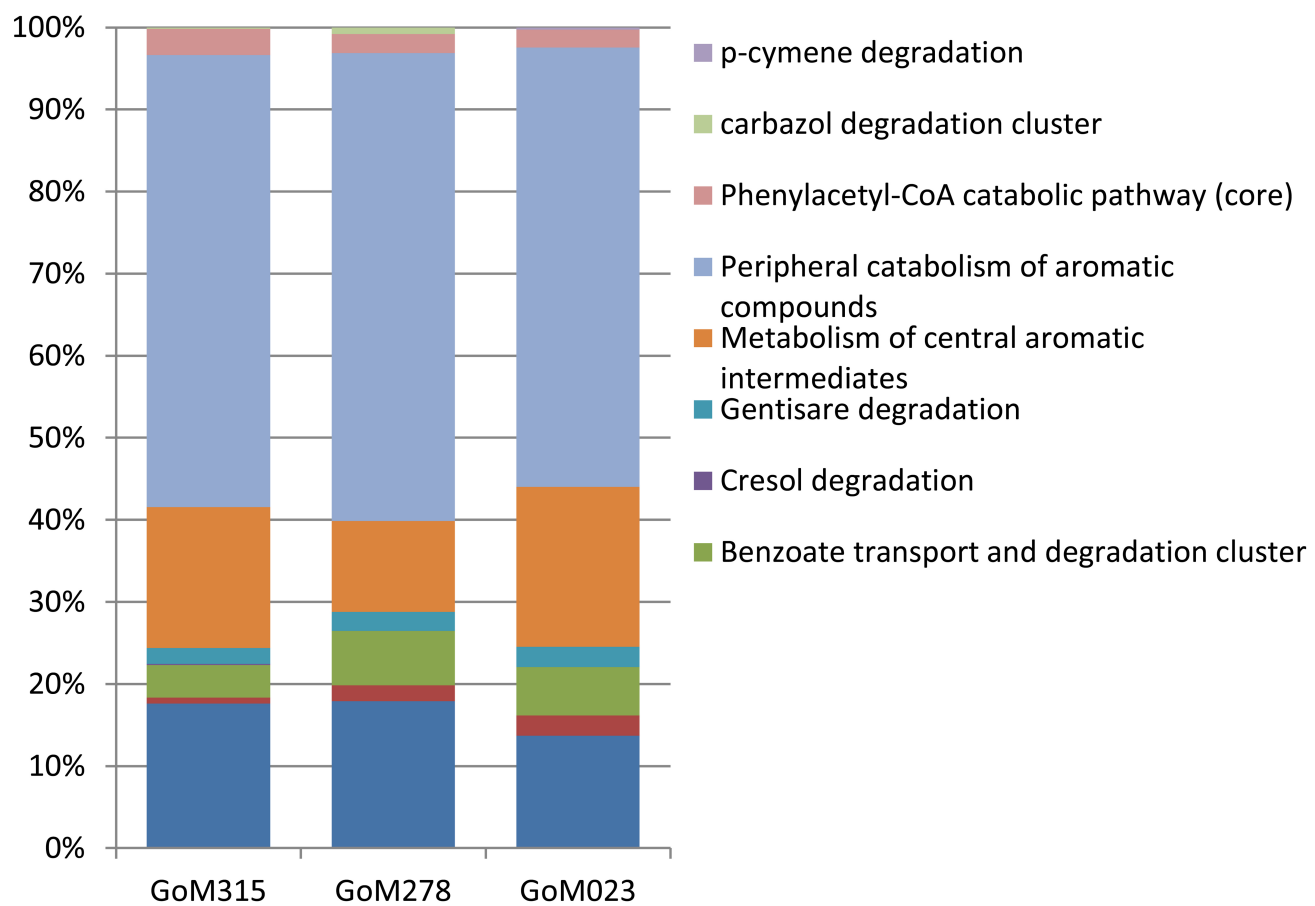


Figure 6.JPEG

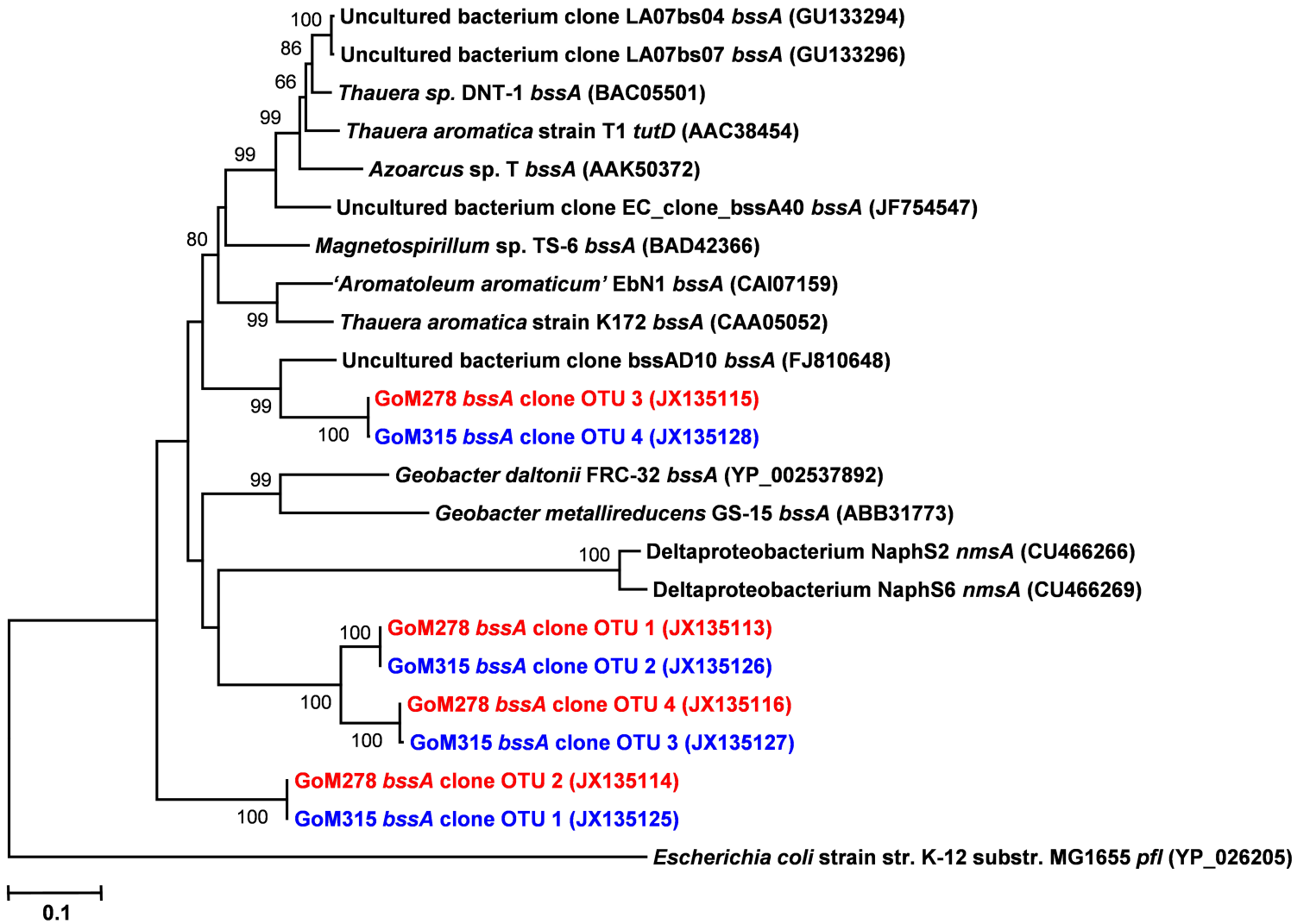


Figure 7.JPEG

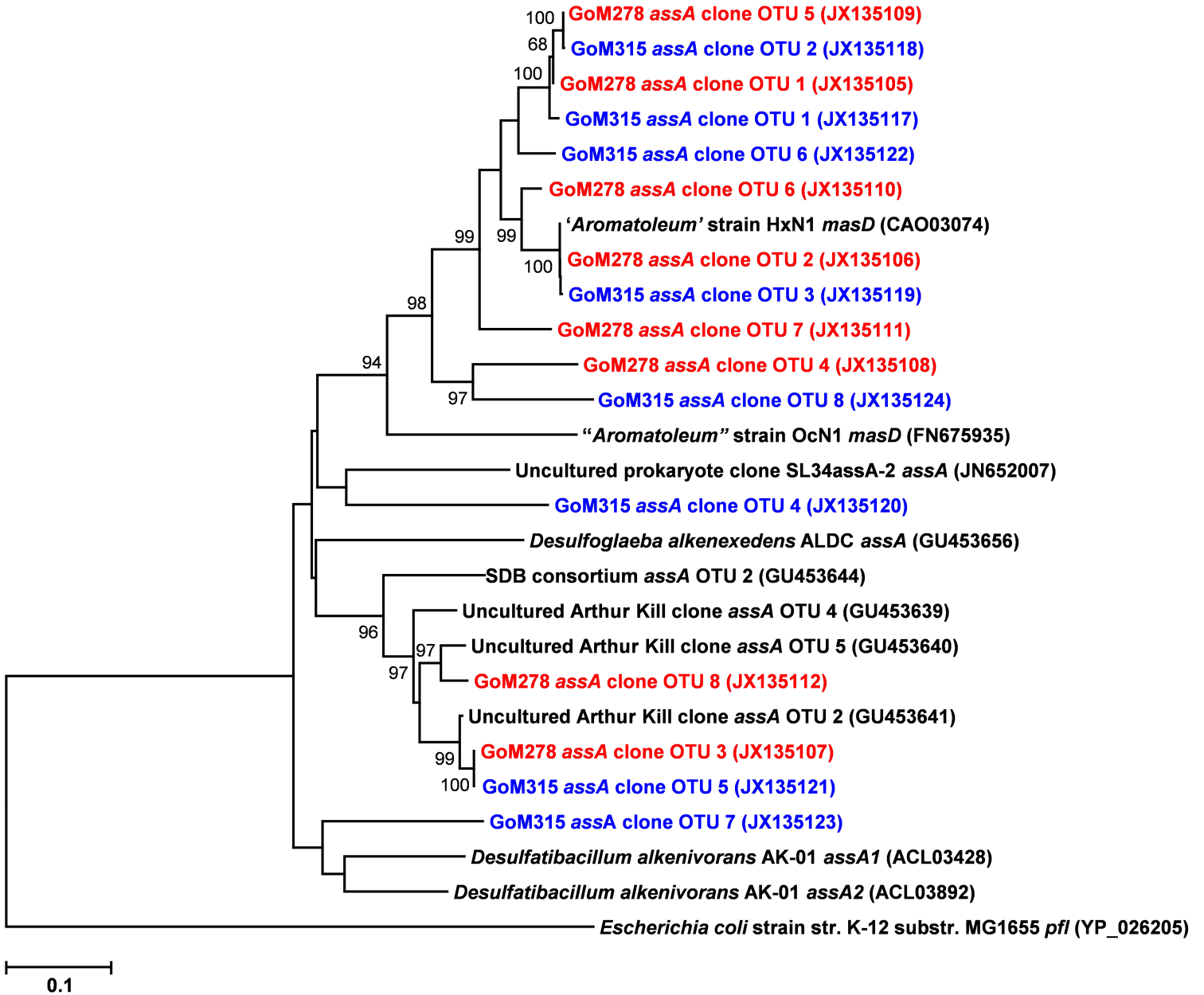


Figure 8.JPEG

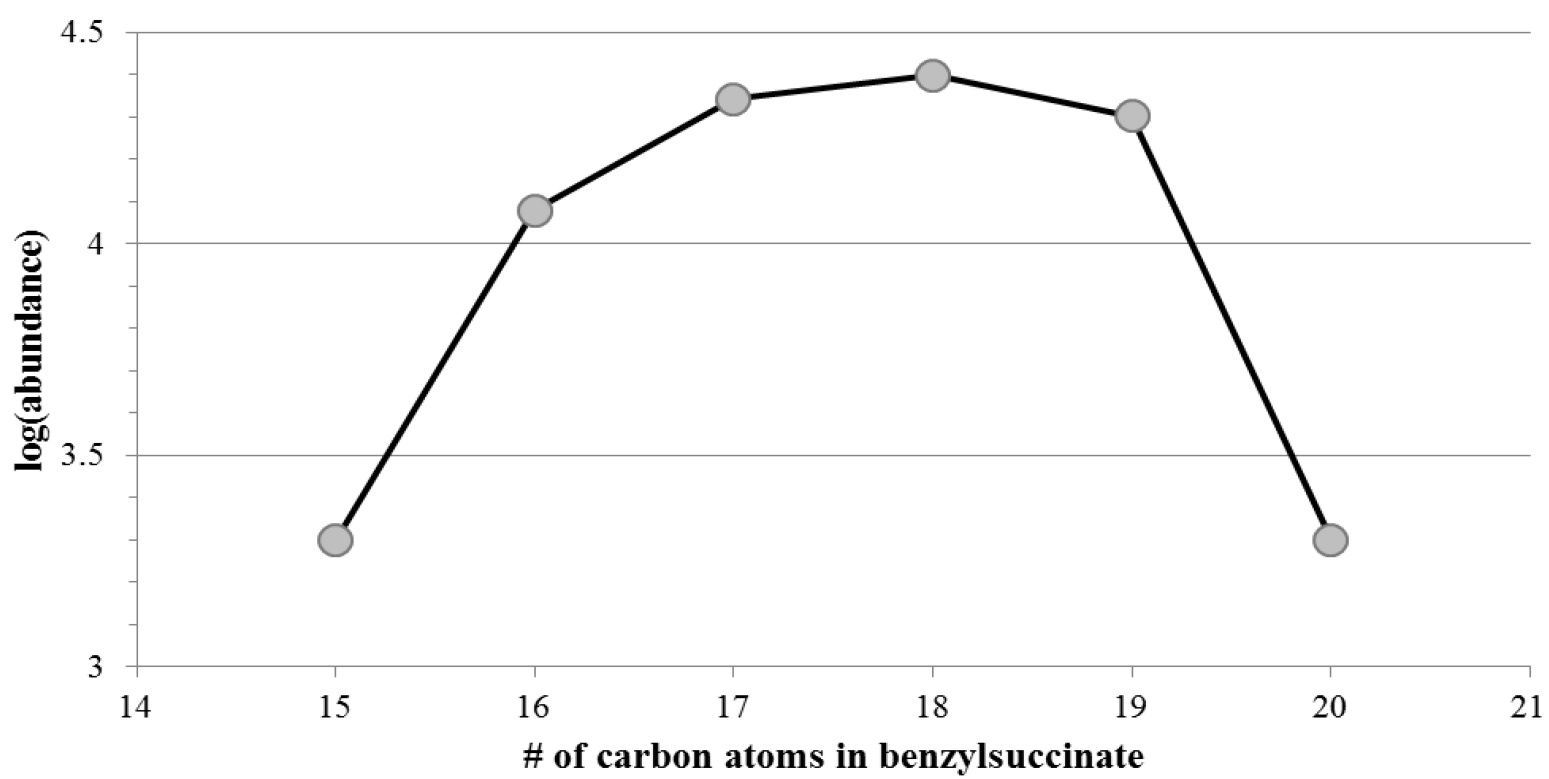


Figure 9.JPEG

